

ANTENNA SIMULATIONS ON SHIPS FOR AMRFS APPLICATIONS

Eighth Quarterly Report

**BAE SYSTEMS
95 Canal Street NCA1-6268
P.O. Box 868
Nashua, NH 030601-0868**

**Erdem Topsakal
Rick Kindt
Kubilay Sertel
John Volakis**

September 2001

Rad Lab Alex

*RL ~~1004~~
1004*

RL-1004 = RL-1004

PROJECT INFORMATION

PROJECT TITLE: ANTENNA SIMULATIONS ON SHIPS FOR AMRFS
APPLICATIONS

REPORT TITLE: 8th Quarterly Report

U-M REPORT No.: 038954-10-T

CONTRACT

START DATE: October 1999

END DATE: March 2002

DATE: September, 2001

SPONSOR: Art E. Dinbergs
BAE SYSTEMS
Mail Stop, MER 15-1351
PO Box 868
Nashua, NH 030601-0868
Phone: (603) 885-8690
Email: arturs.e.dinbergs@baesystems.com

Quarterly Reports Quarterly Reports
James F. Long
BAE SYSTEMS
MER 15-2516
130 DW Highway, North
Merrimack, NH 03054
Phone:(603) 885-4460
Fax :(603) 885-4189
james.f.long@baesystems.com

SPONSOR

CONTRACT No.: RF5443

U-M PRINCIPAL

INVESTIGATOR: John L. Volakis
EECS Dept.
University of Michigan
1301 Beal Ave
Ann Arbor, MI 48109-2122
Phone: (313) 764-0500 FAX: (313) 747-2106
volakis@umich.edu
<http://www-personal.engin.umich.edu/~volakis/>

CONTRIBUTORS TO THIS REPORT: Erdem Topsakal, John Volakis







TABLE OF CONTENTS

TABLE OF CONTENTS.....	3
CHRONOLOGY of EVENTS	4
QUARTERLY PROGRESS.....	5
DETAILED SCHEDULE (October 1999-December 2000).....	7
DETAILED SCHEDULE (December 2000-December 2001).....	9
EXECUTIVE SUMMARY AND PROJECT STATUS.....	10
AMFIA UPGRADES.....	11
EXAMPLE LOADED PATCH	11
SOLVERS AND PRECONDITIONERS	13
LARGE FINITE LTSA ARRAYS	20
EXAMPLE 4x3 LTSA AARRAY	20
EXAMPLE 6x6 LTSAA ARRAY	22
SHIP TOWER WITH ANTENNAS	24
COUPLING STUDIES	25
REFERENCES.....	31

CHRONOLOGY of Events (Updated Every Quarter)

- October 1998 Proposal Submission
- December 1998 Oral Presentation to ONR
- August 1999 Began Contract Negotiations
- 26 August. 1999 Kickoff meeting at Sanders (attended by Sanders, UM , ONR)
- 13 October 1999 Contract Signed between U-M and Sanders
- 18 October 1999 MR_TETRA Code and the manual delivery
- 15 December 1999 Submission of First Quarterly Report
- 19 January 2000 AMRFS Review Meeting I (Lockheed Sanders - Nashua)
- 19 January 2000 ARRAY_TETRA Code delivery
- 1 April 2000 Submission of Second Quarterly Report
- 15 June 2000 Submission of Third Quarterly Report
- 27 July 2000 AMRFS Review Meeting II (Lockheed Sanders – Nashua)
- 15 September 2000 Submission of Fourth Quarterly Report
- 15 December 2000 Submission of Fifth Quarterly Report
- 24 January 2001 AMRFS Review Meeting III (BAE Systems – Nashua)
- 15 March 2001 Submission of Sixth Quarterly Report
- 15 June 2001 Submission of Seventh Quarterly Report
- 26 July 2001 AMRFS Review Meeting IV(BAE Systems – Nashua)
- 15 September 2001 Submission of Eighth Quarterly Report

Quarterly Progress

Task	1 st	2 nd	3 rd	4 th
Implementation of the Periodic Boundary Conditions in MR_TETRA				
Fast Spectral Domain Algorithm Applied to MR_TETRA (AIM delivered at this time)				
Finite Arrays / MR_TETRA_F Implementation and Formulation				
F77 to F90 code inversion for MR_TETRA_F And Code Optimization				
Coupling Studies between Elements and Array groups				
FMM_FSS_CURVE code initiation				

Task	5th	6th	7th	8th
<i>ARRAY_TETRA</i> delivery				
Implementation of the Periodic Boundary Conditions in FSS-CURVE –(3rd year)				
Implementation of Multilevel FMM in FSS-CURVE				
Coupling Implementation Elements and Array groups				
Code Optimization and Testing				
<i>FSS_CURVE</i> delivery				

DETAILED SCHEDULE (October 1999-December 2000)

No.	Description	Due Date
1	FSS_PRISM updated with Tetrahedral FEM(<i>MR_TETRA</i>) Accelerated with Adaptive Integral Method Code and the Manual	DELIVERED (1st)
2	<p>a) Periodic Boundary Conditions Implementation and validation</p> <p>b) <i>ARRAY_TETRA</i> Code</p> <p>c) Finite element approximation</p> <hr/> <p>d) Convert F77 to F90 (final modifications)</p> <p>e) Array coupling formulation</p> <p>Added Task:</p> <p>f) Validations for patch and slot arrays IDEAS/PATRAN/GID interface</p>	<p>COMPLETE</p> <p>DELIVERED (2nd)</p> <p>COMPLETE</p> <hr/> <p>ONGOING</p> <p>COMPLETE</p> <p>COMPLETE</p>
3	<p>a) FSS-Curve updated with MLFMM BI and hexahedral FEM</p> <p>b) External field coupling (plane wave)</p>	<p>COMPLETE</p> <p>COMPLETE</p>

	f) LTSA mesh driver e) LTSA and ETSA validations	COMPLETE COMPLETE
4	a) Demonstrate fully documented ARRAY_TETRA Version 2 (all tasks except coupling to be completed in this version of the code) b) Update FSS-Curve for tetrahedral elements –removed task c) Implement Periodic boundary conditions in FSS_CURVE (added task)-3 rd year	September. 2000 DELIVERED (see manual for the code information)
5	a) Coupling studies and realistic array analysis for FSS_CURVE (AMFIA) (edge diffraction effects, element grouping etc) b) Demonstrate fully documented FSS-CURVE First Release	December. 2000 ONGOING DELIVERED

DETAILED SCHEDULE (December 2000-December 2001)

No.	Description	Due Date
1	<p><u>Remaining ARRAY TETRA modifications</u></p> <p>1) BCs and Feeds in Patran</p> <p>2) FSDA</p> <p>3) Arbitrary external excitations</p> <p>4) Pins and Loads</p> <p>4) F90 version</p> <p><u>ARRAY -TETRA final release (F90)</u></p> <p><u>AMFIA Modifications</u></p> <p>1) I/O modifications</p> <p>2) Initial User's Manual</p> <p>3) MLFMM implementation</p> <p><u>AMFIA first release (f77)</u></p> <p>5) Coupling in a finite array environment</p>	<p style="text-align: center;">COMPLETED</p> <p style="text-align: center;">ONGOING (July 2001)</p> <p style="text-align: center;">ONGOING (July 2001)</p> <p style="text-align: center;">ONGOING (July 2001)</p> <p style="text-align: center;">ONGOING (December 2001)</p> <p style="text-align: center;">December 2001</p> <p style="text-align: center;">COMPLETED</p> <p style="text-align: center;">COMPLETED</p> <p style="text-align: center;">COMPLETED</p> <p style="text-align: center;">DELIVERED</p> <p style="text-align: center;">December 2001</p>

Executive Summary and Project Status

We continue to be on schedule with all activities and code development tasks. In the fourth project review at Sanders (in July 2001), we presented results for finite arrays (patch, slot and TSAs (Tapered Slot Arrays)) using our AMFIA code. We also presented coupling results between antenna array elements and subarray-subarray. We also demonstrated some primary results using our newly developed, highly robust and exact AMFIA code. New code also upgraded from F77 to F90.

Besides the coupling studies we demonstrated in the last review, this quarter we also focused on enriching the solver capabilities in AMFIA. A new solver BICGS(L) (Biconjugate gradient solver with respect to parameter L) has been shown to give better convergence characteristics compared to CGS, QMR and BICG for TSAs. An example of microstrip fed TSA antenna is given to demonstrate the performance of different solvers.

Another update in this quarter was the addition of a term to FE-BI formulation which is used when loads and shorting pins presents. A microstrip patch antenna has been chosen [1] to validate the results.

During this quarter no changes were made to ARRAY_TETRA. The final f77 version of ARRAY_TETRA will be delivered to BAE December 20th after remaining modifications (outlined in the last report—Executive Summary and Project Status) are completed. F90 version of ARRAY_TETRA will also be available by that time.

In the last report, we also gave some coupling results using our newly developed AMFIA code.

To summarize, the tasks carried out this quarter are;

- Formulation and Implementation (Shorting pins and Loads for AMFIA)
- Implementation of a new solver BICG(L) and comparison with the existing solvers for TSA
- Coupling between array groups
- Large finite arrays

For the next quarter our goals are;

- Formulation details and implementation outlines of Super Cell
- FSDA for ARRAY_TETRA with validations
- F90 version of ARRAY_TETRA

AMFIA UPGRADES

Several upgrades have been carried out for AMFIA this quarter. We first modified the existing formulation to treat loads and shorting pins in the geometry. Below we provide a microstrip patch antenna example for validation of this implementation. Another modification was the inclusion of a new solver. We show here that the new solver has increased the convergence substantially. To demonstrate the solver, we analyzed a microstrip-fed LTSA and compared convergence with the other solvers

EXAMPLE-Microstrip Patch Antenna

As an example for the validation of the loads and shorting pins, we consider the microstrip patch antenna displayed in Fig.1. Input impedance characteristics of this antenna were computed from 1-4GHz. Figure 2 shows the input impedance for the antenna when a 50Ω resistor is placed at $(x=-2,2 \text{ cm}, y=-1.5\text{cm})$. As seen our calculations compare well with measurements [1].

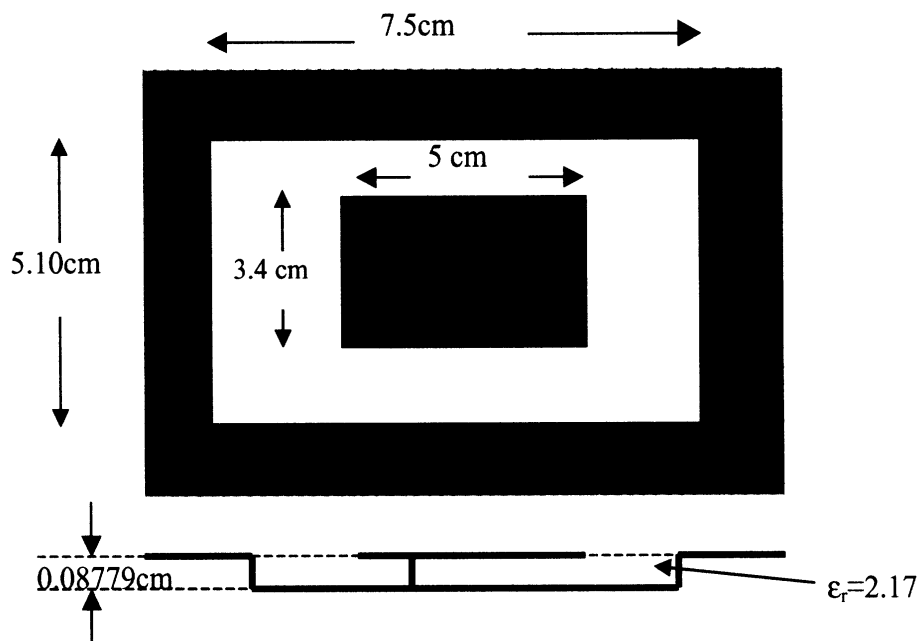


Figure 1. Microstrip Patch Antenna Geometry

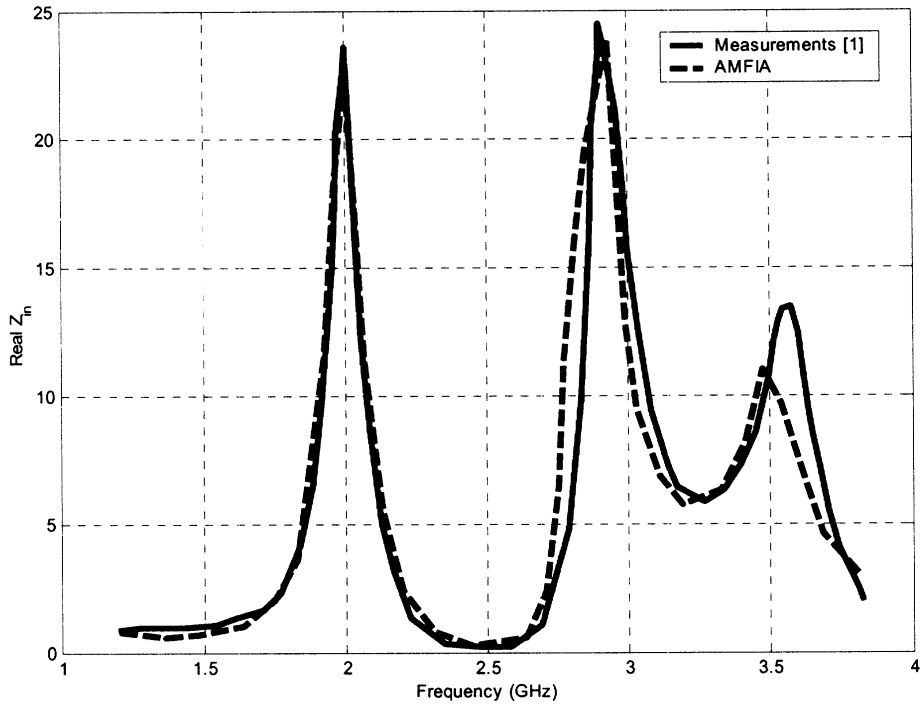


Figure 2. Input Impedance Validation (Real Part)

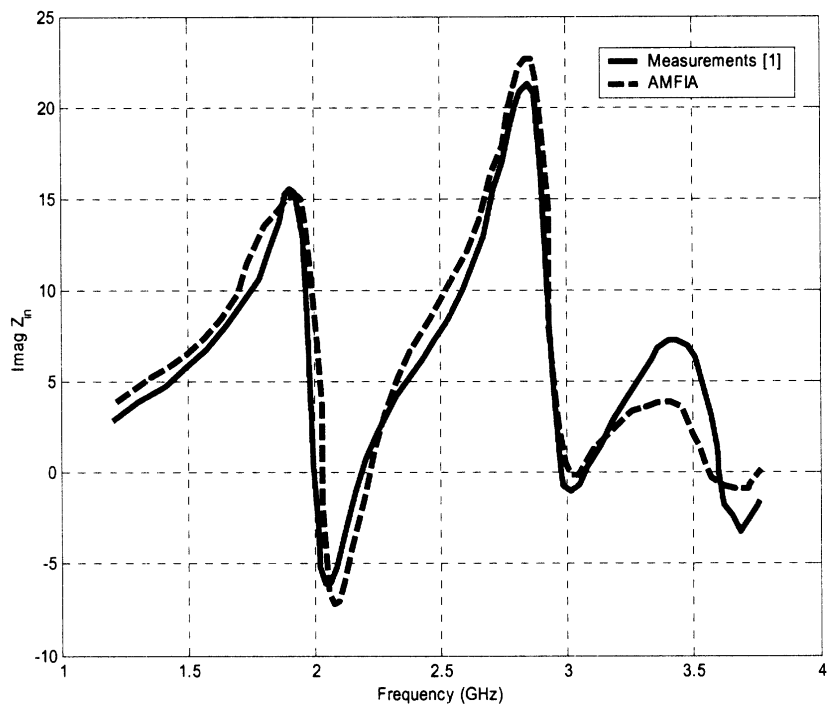


Figure 3. Input Impedance Validation (Imaginary Part)

SOLVERS AND PRECONDITIONERS

This quarter we also investigated the convergence behavior of different solvers and preconditioners for TSAs. For this purpose 4 solvers and 2 preconditioners were analyzed.

Solvers:

- QMR (Quasi-Minimal Residual)
- CGS (Conjugate Gradient Squared)
- BICG (Bi-conjugate Gradient)
- BICGS (L) (Bi-conjugate stabilized with respect to L)

Preconditioners:

- Diagonal
- ILU (Incomplete LU)

We are not going to go into details of these methods here. References can be found in the literature. (QMR,CGS,BICG and Preconditioners [2],[3], BICGS(L) [4]). To see the performance of those solvers and preconditioners, we consider a microstrip fed LTSA antenna operating at 10GHz (see fig 4).

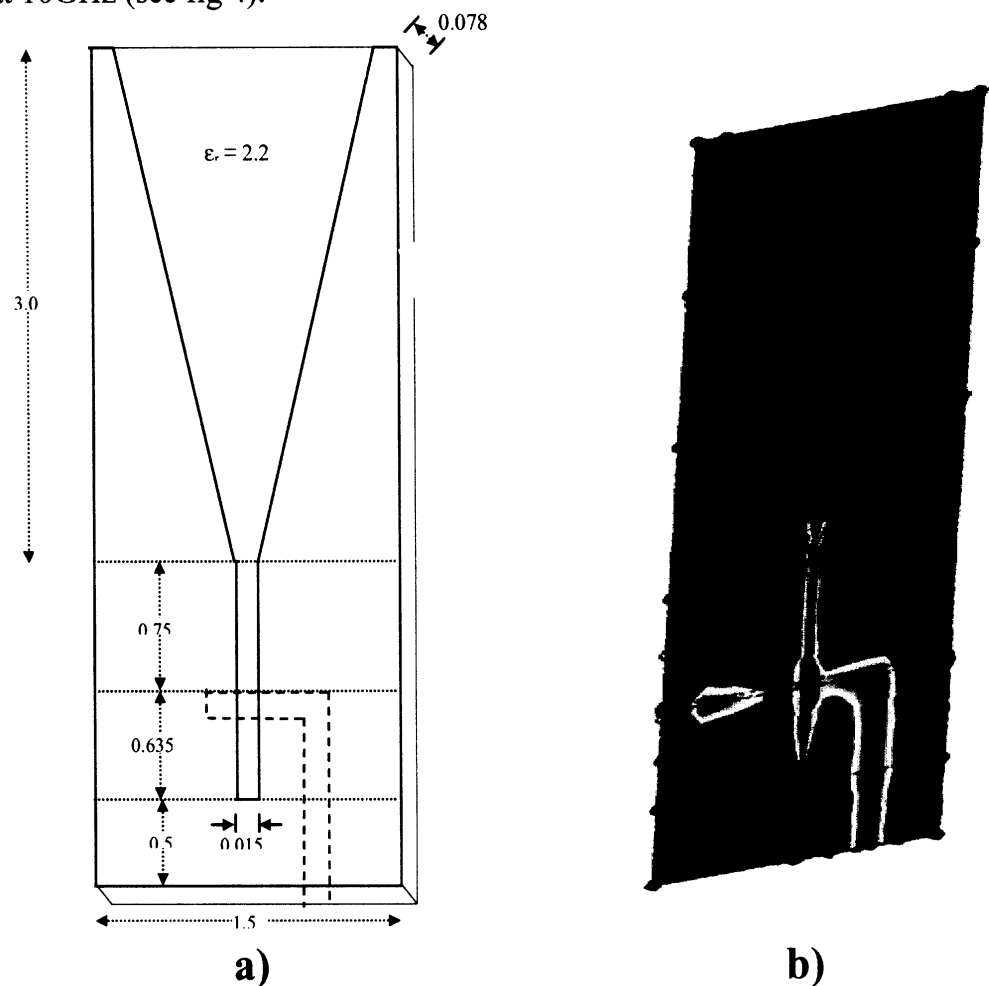


Figure 4. a) Microstrip-fed antenna geometry b) Field Distribution

Figs. 5&6 show the field patterns for E&H plane cuts from 8-12 GHz. As seen the data are not symmetric due to non-symmetric feeding (see fig.4a).

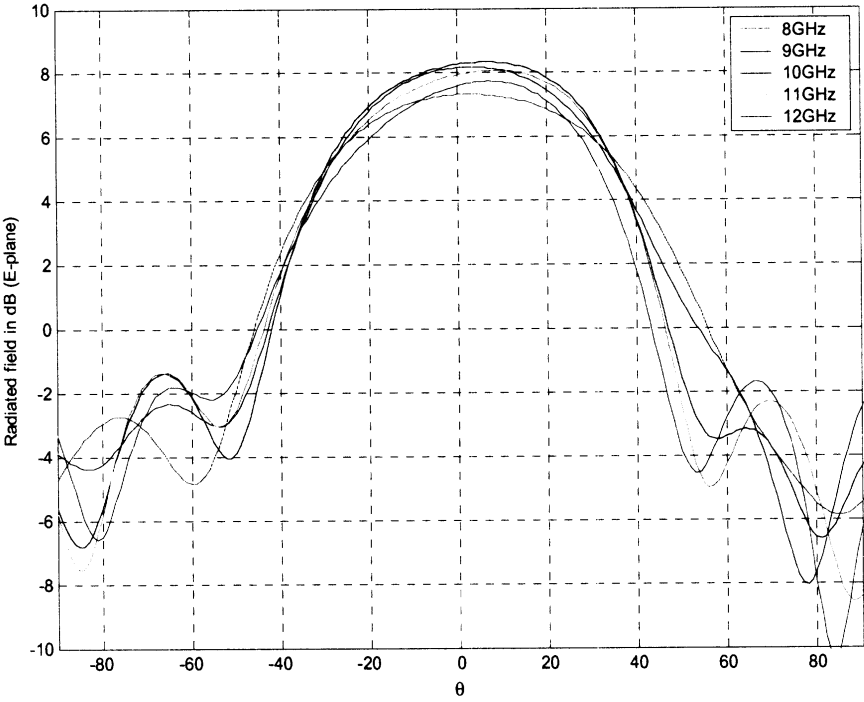


Figure 5. Radiated Field versus observation angle–(E-plane)

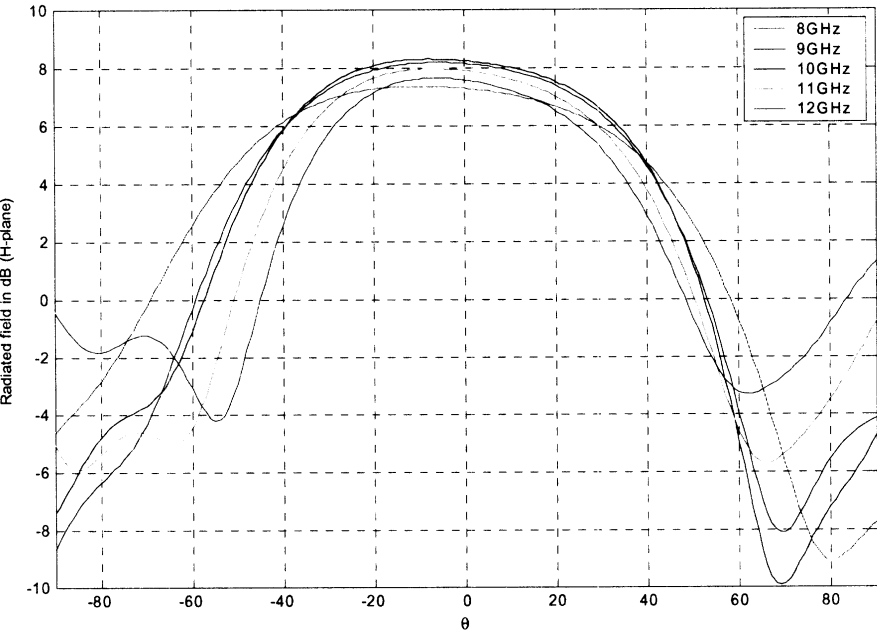


Figure 6. Radiated Field versus observation angle–(H-plane)

Figs. 7-9 show the convergence behavior of the solvers used in AMFIA for the microstrip fed LTSA antenna. In Fig. 7 no preconditioners are used. In Figs 8,9 diagonal and ILU preconditioners are used. As seen, BICGSTAB(L) has substantially better convergence behavior compared to the other solvers. It converges almost 10 times faster in all cases compared to the closest converged solver.

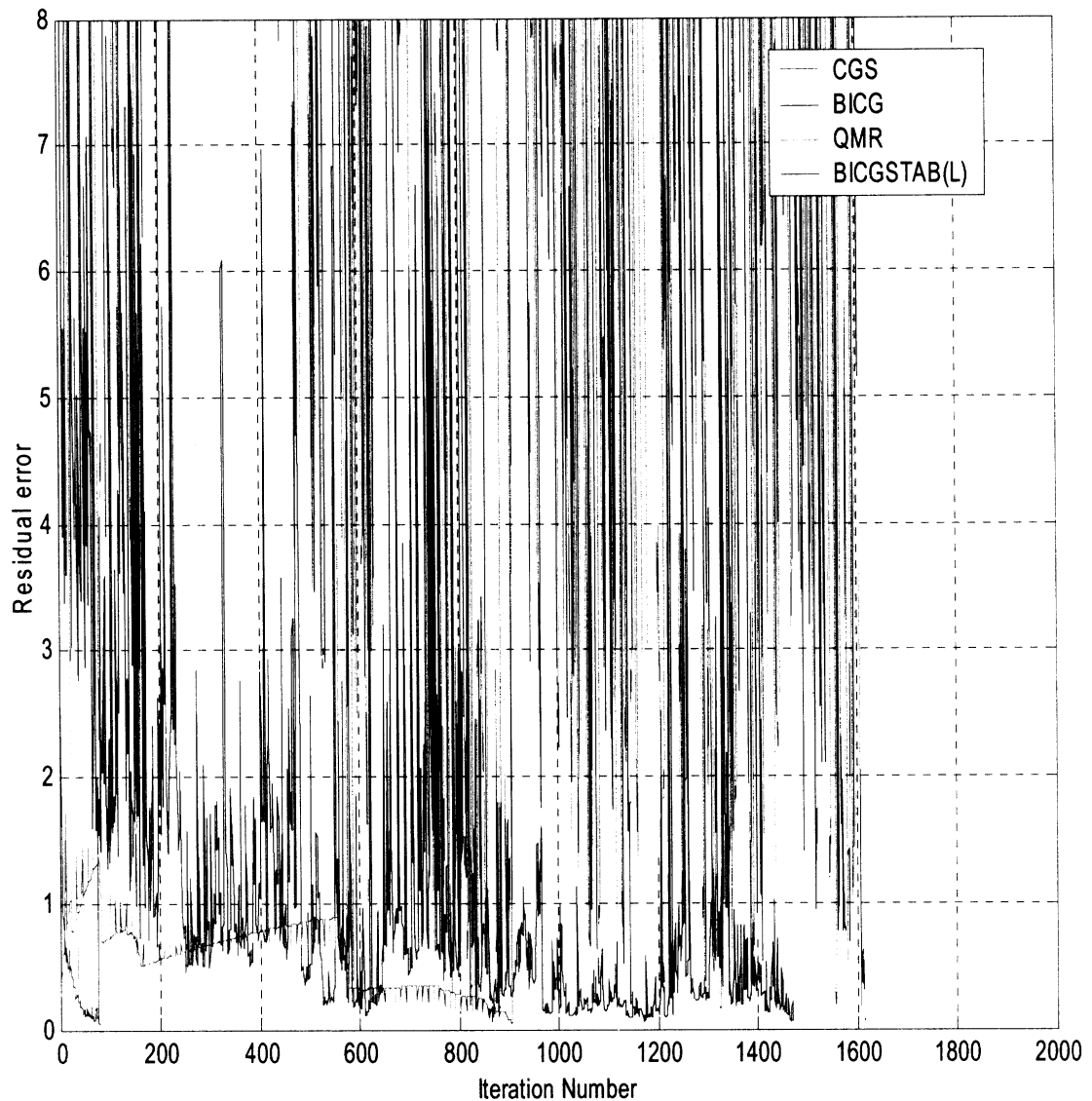


Figure 7. Solvers convergence behavior (no pc)

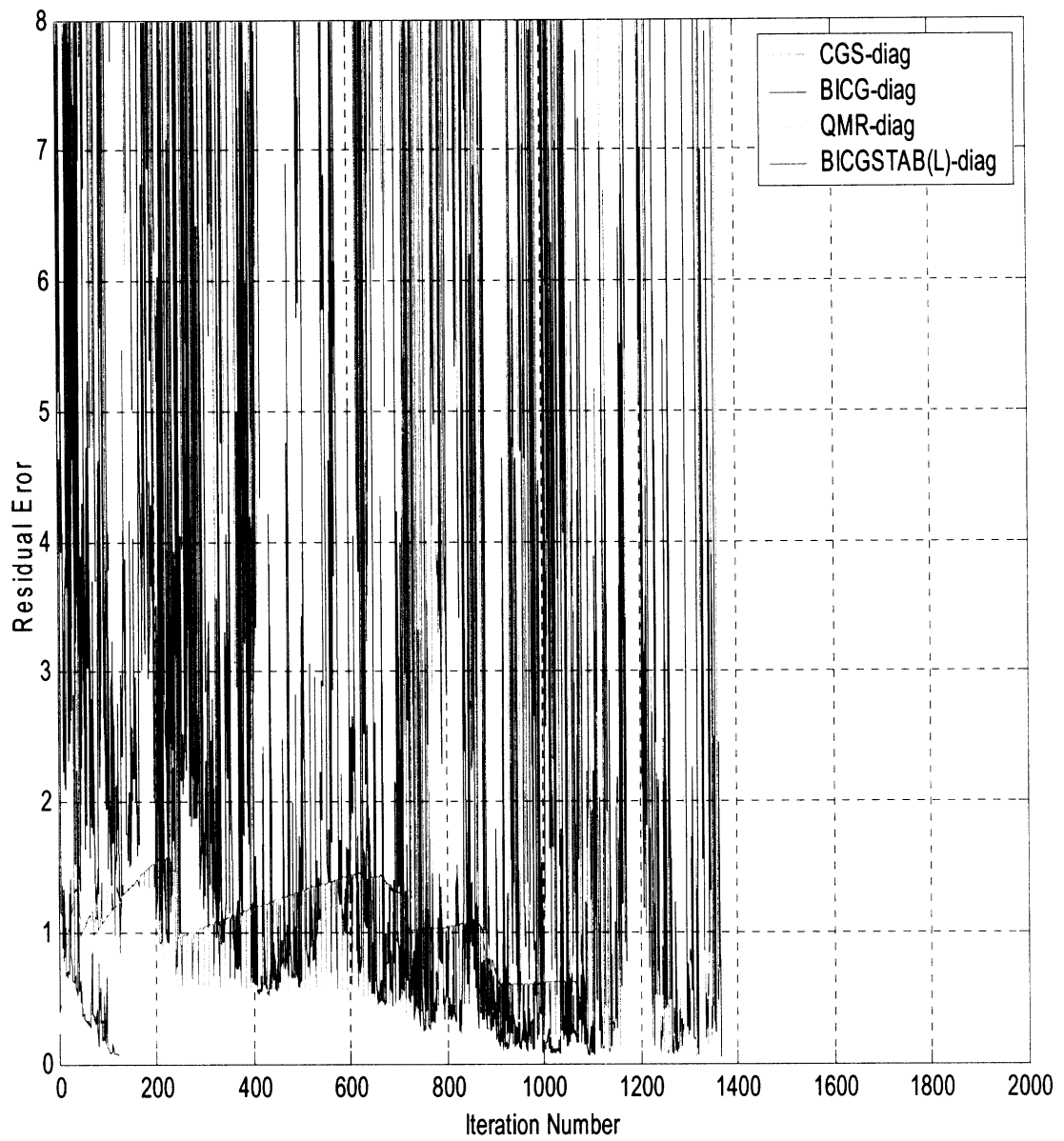


Figure 8. Solvers convergence behavior (Diagonal Preconditioner)

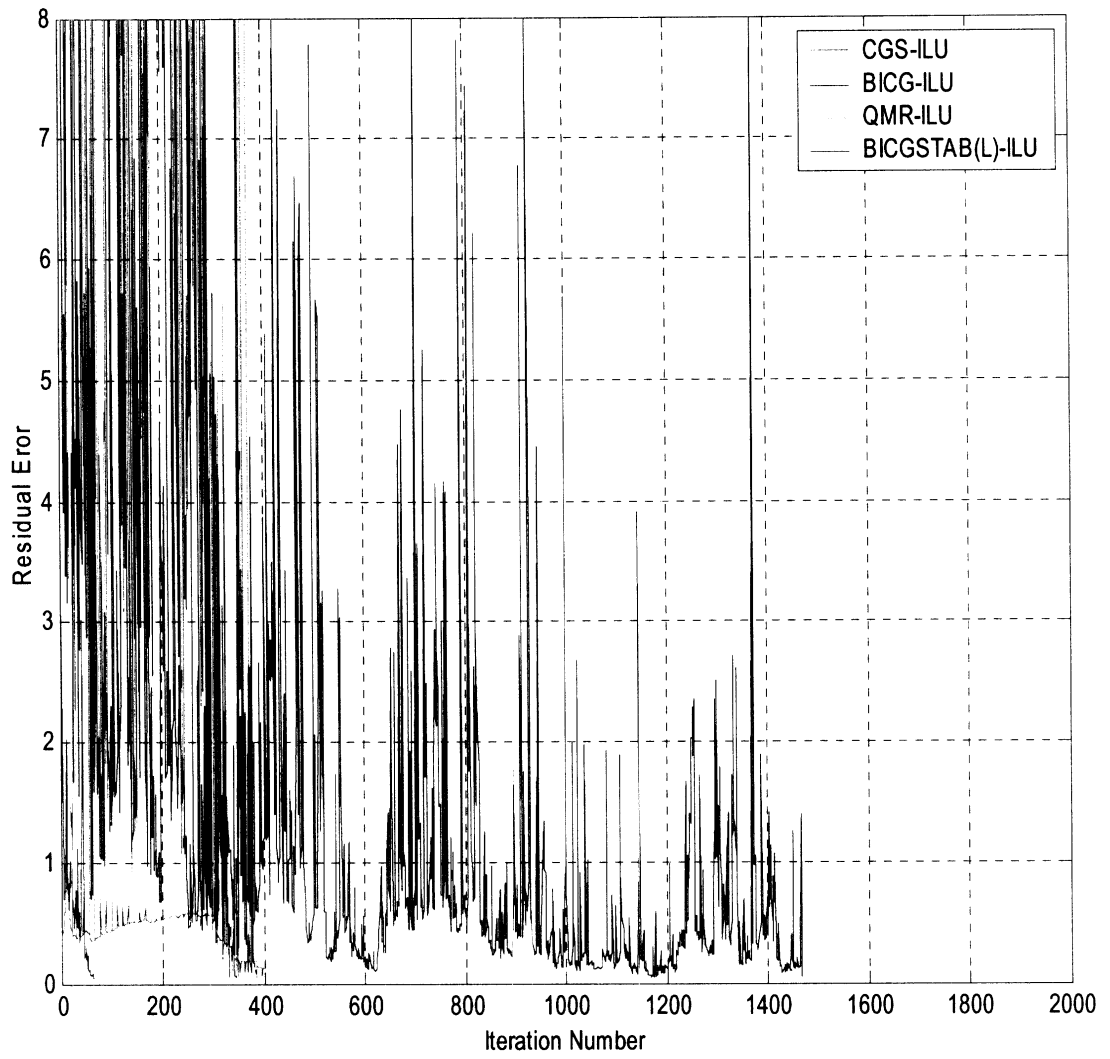


Figure 9. Solvers convergence behavior (ILU)

Figs. 10-12 show the effect of the “L” parameter for BICGSTAB(L) solver for various preconditioners. In all cases, iteration number decreases with increasing “L” value. However for values of “L” greater than “5”, decrease in the iteration number slows down.

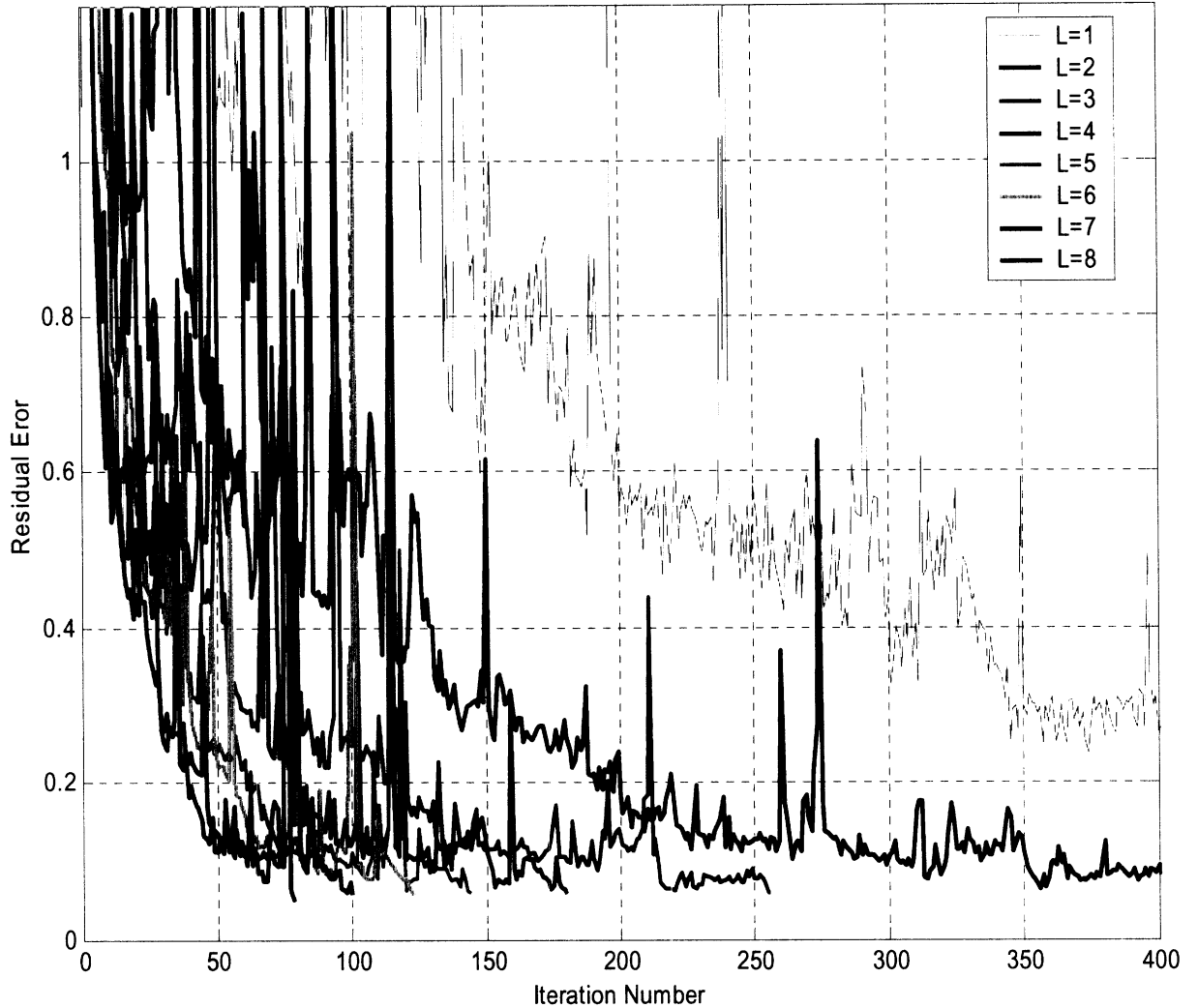


Figure 10. Effect of L parameter (nopc)

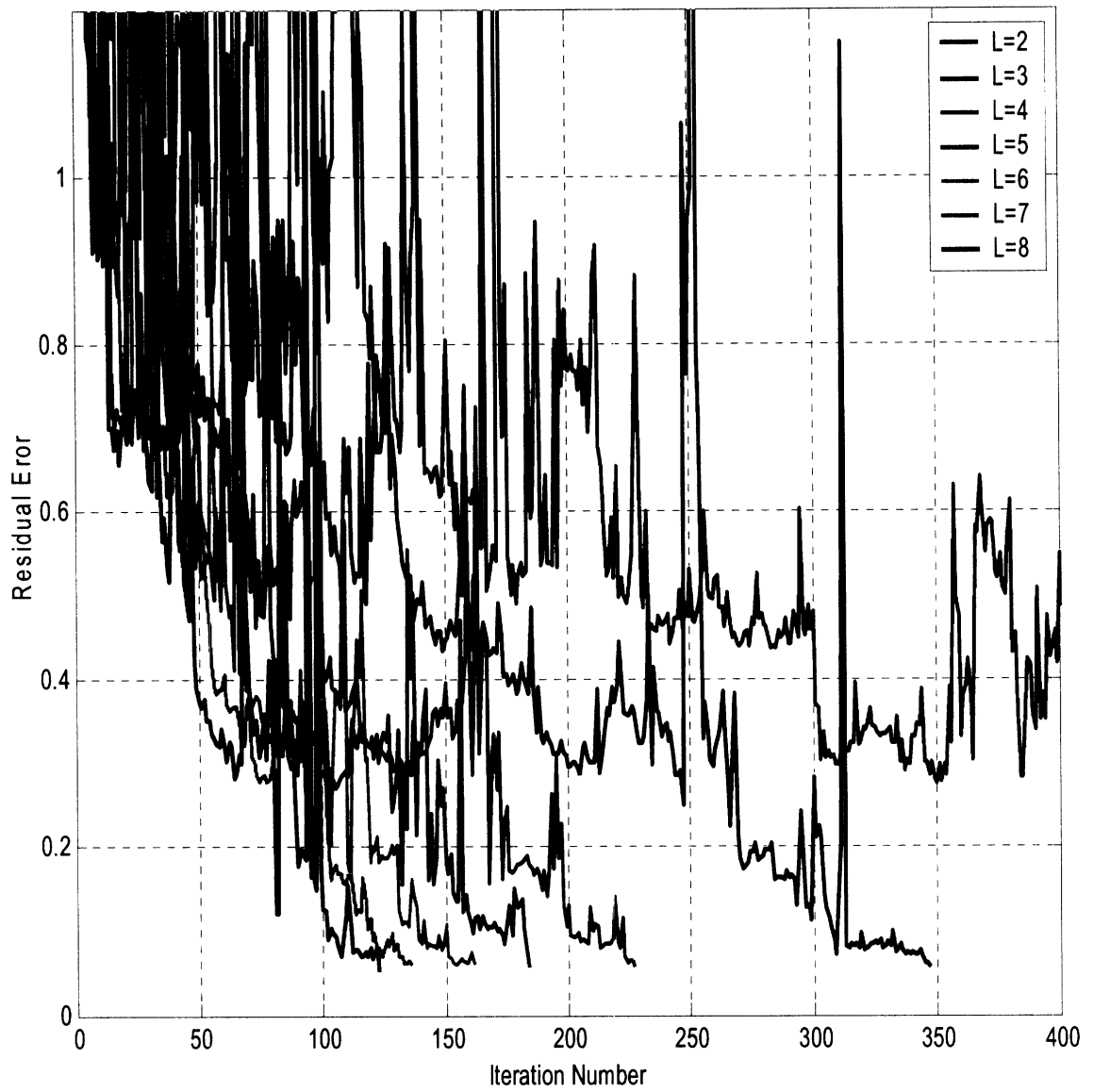


Figure 11. Effect of L parameter (Diagonal Preconditioner)

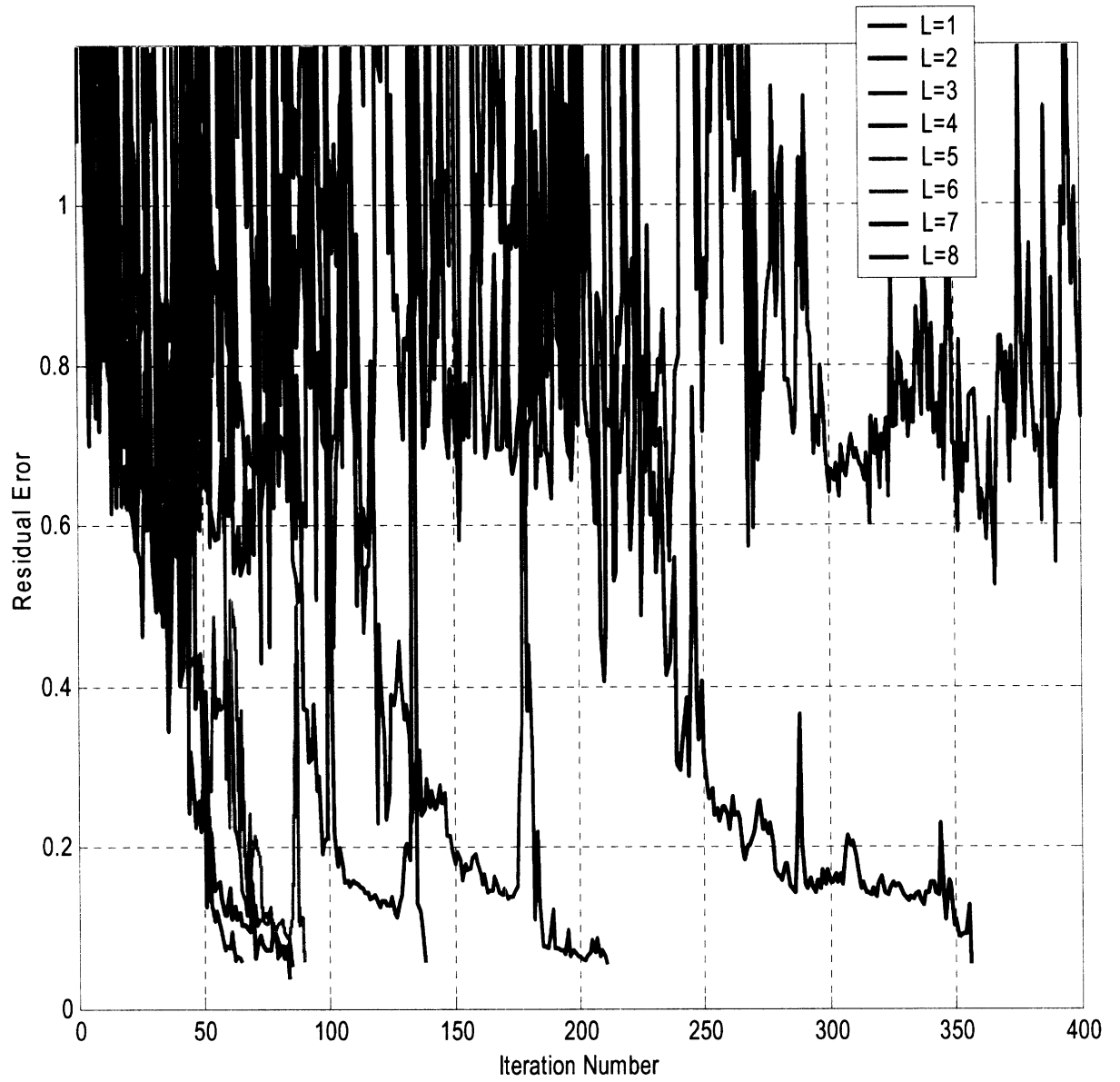


Figure 12. Effect of L parameter (ILU)

Large Finite LTSA arrays

a) 4x3 LTSA array

Consider the 4x3 LTSA shown in fig. 13b. All array elements are identical and the dimensions are given in Figure 13a. The slotline feed is designed to be 100 ohms at 10GHz and the feed point is positioned 0.635cm from the slotline short. The antenna is 4.885cm in length.

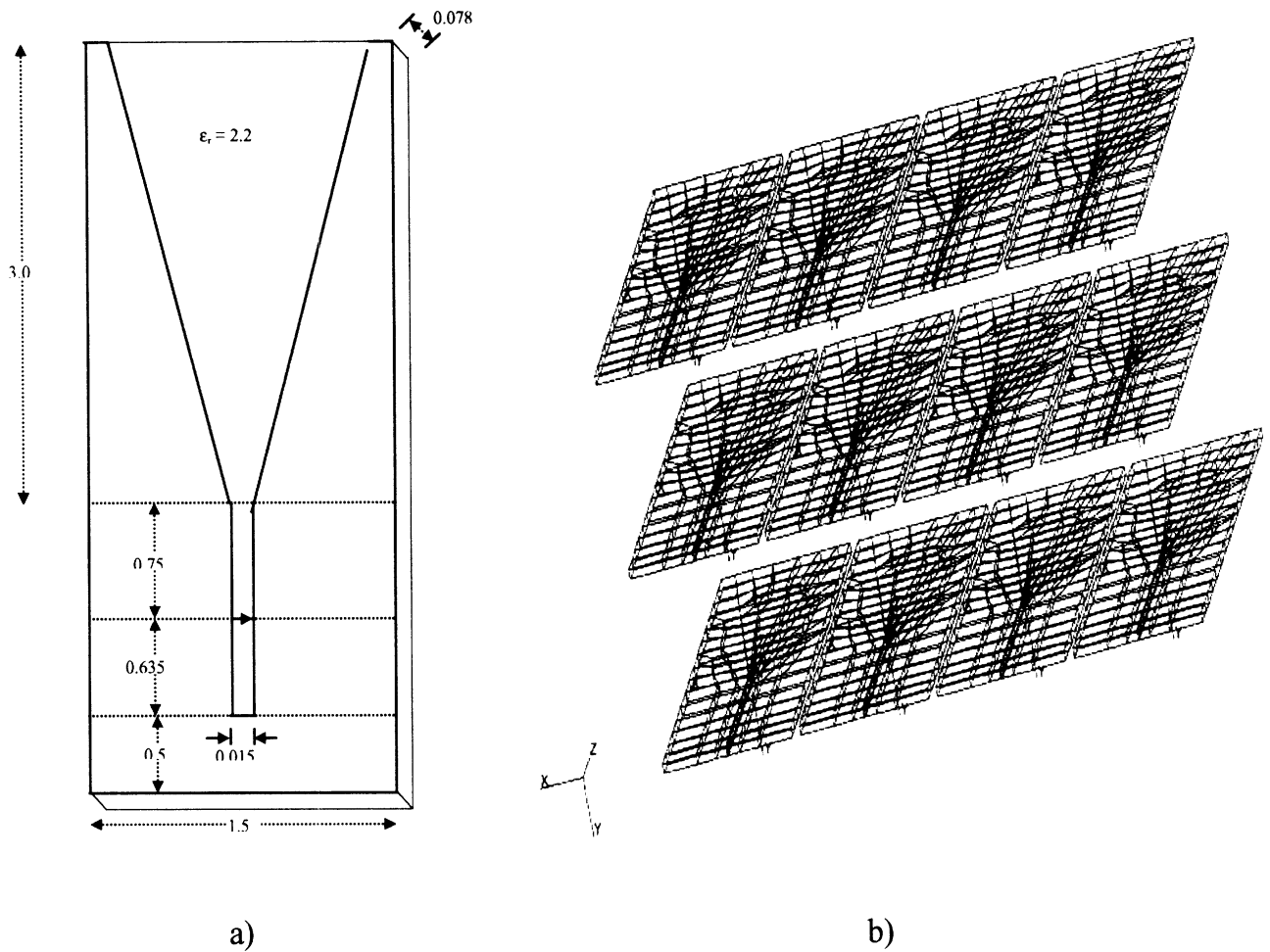


Figure 13 a) Element geometry b) 4x3 array

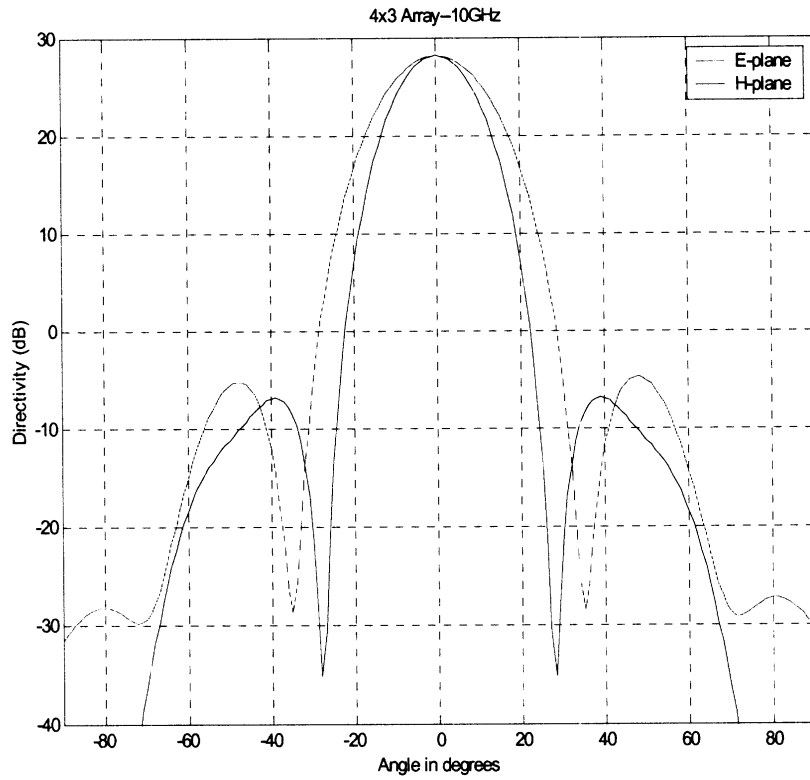


Figure 14. Directivity

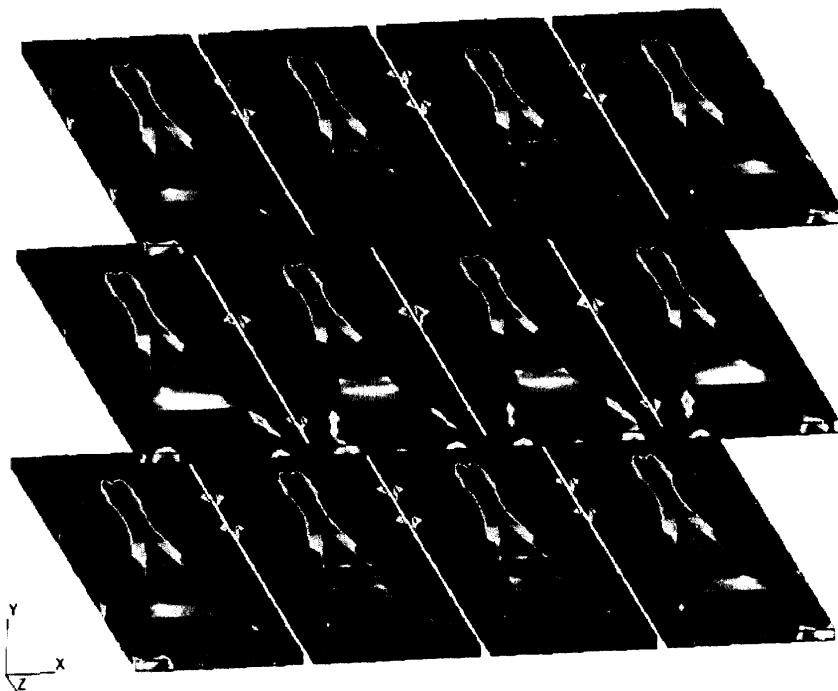


Figure 15. Field distribution on 4x3 array

b) 6x6 LTSA array

Consider the 6x6 LTSA array. All array elements are identical and the dimensions are given in Figure 13a. This problem was solved using 4 level FMM with **800 MB of memory**. Without FMM **10 GB of memory** is required and thus a parallel machine is required to carry out the analysis.

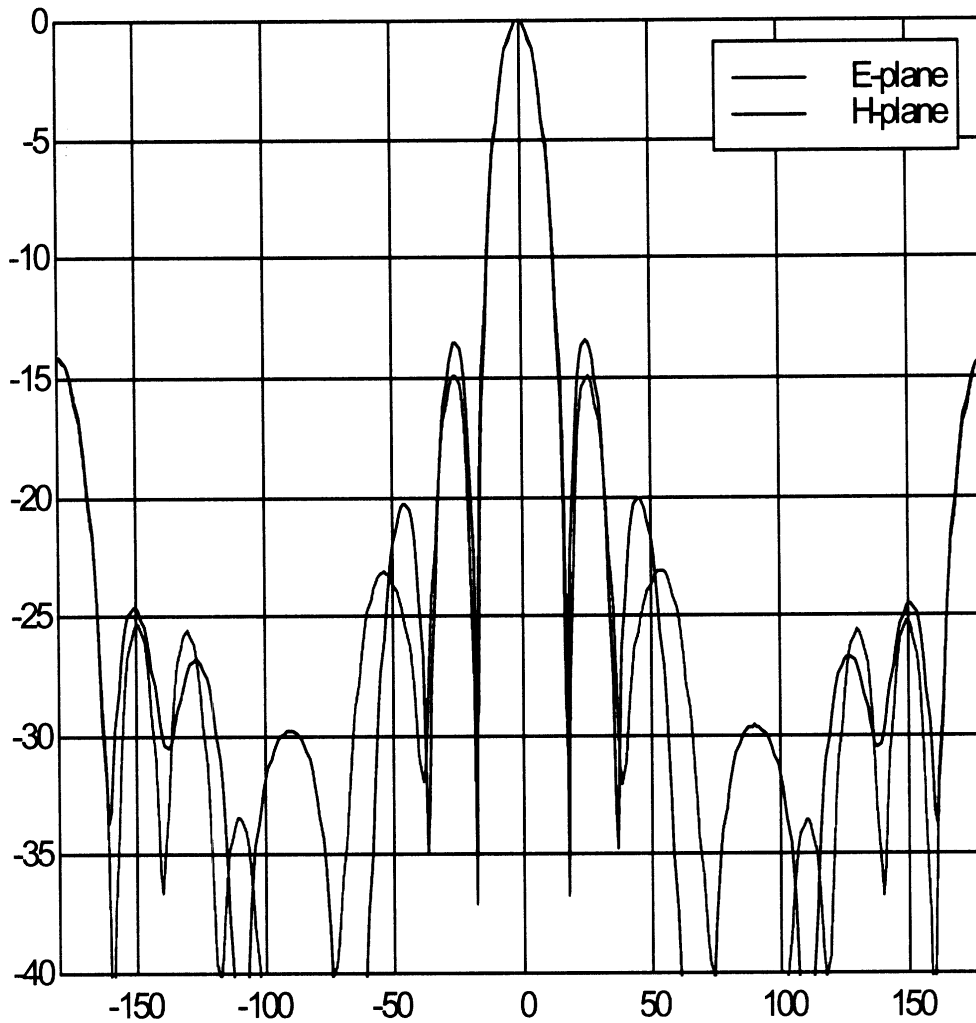


Figure 16. Radiated Fields as a function of observation angle

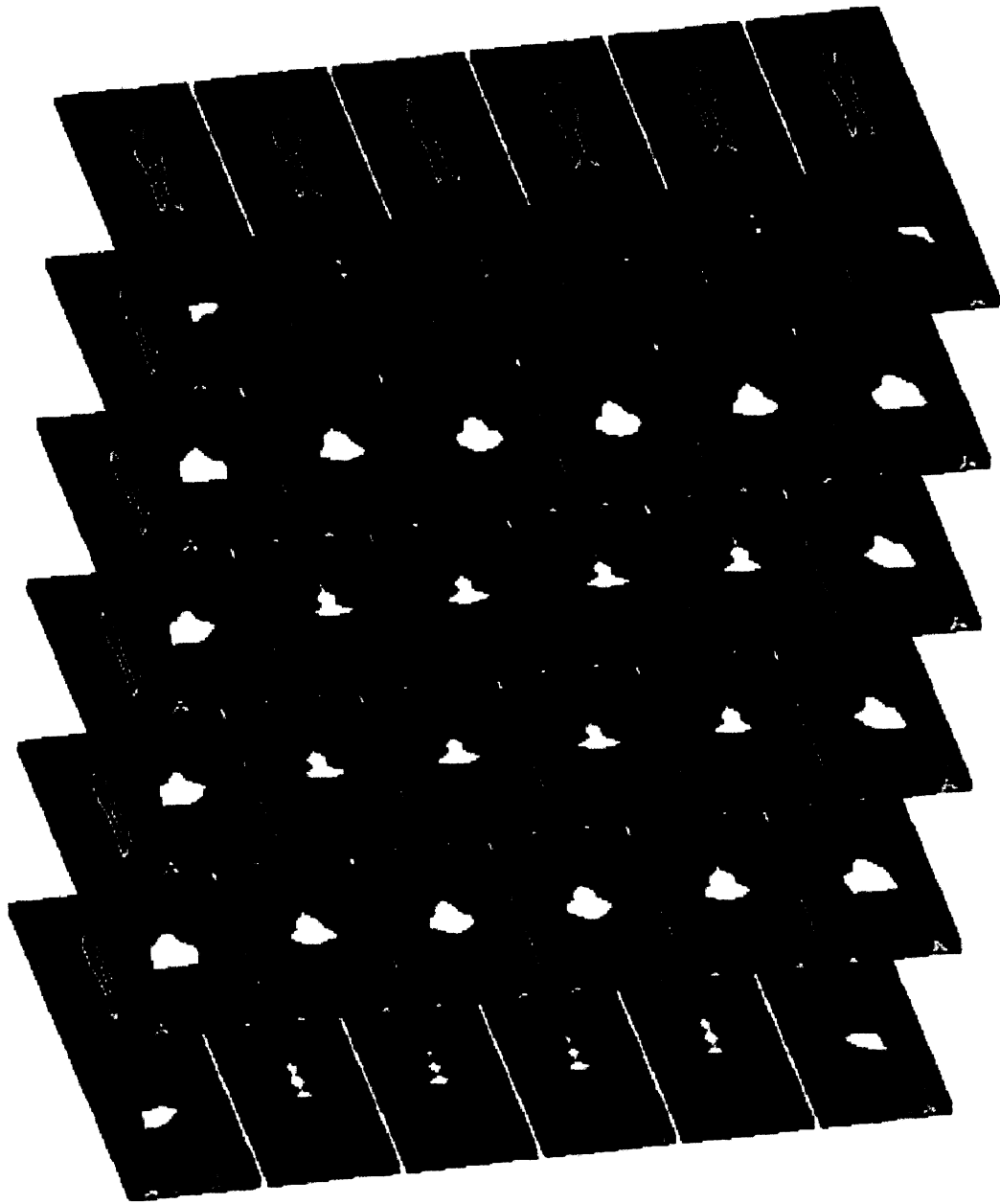
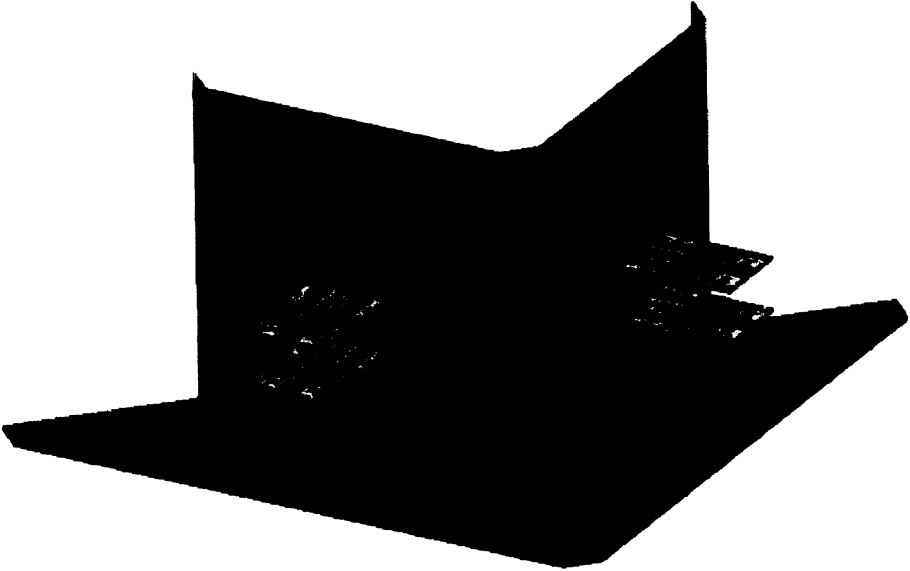


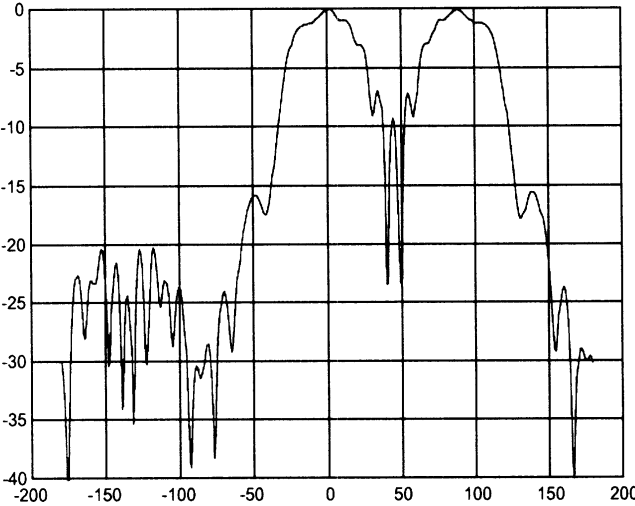
Figure 17. Field distribution

Ship Tower

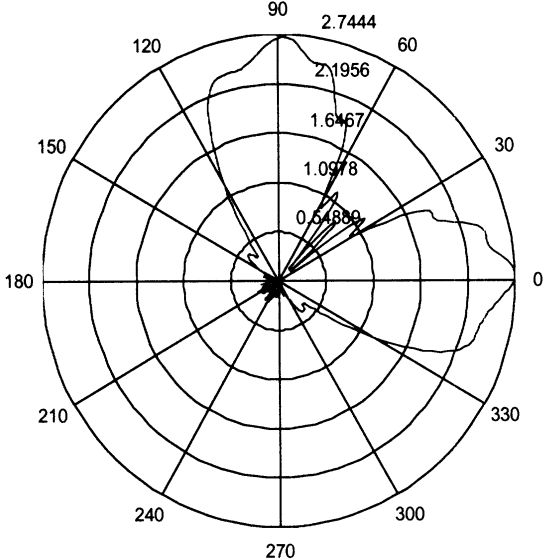
To demonstrate the capabilities of AMFIA we consider the geometry in Fig. 18a. LTSAs are the same ones used in our previous example (see Fig 13a). This problem required only 187Mbytes of memory with 6 level FMM. Without FMM the required memory was 4.3 GB (i.e. 23 times larger).



a)



b)



c)

Figure 18. a) Field distribution b) Radiated Field versus observation angle c) Radiated Field versus observation angle (polar coordinates)

COUPLING STUDIES

In the previous reports we studied element to element coupling within the same array environment this quarter we are expanding our analysis to subarray/subarray coupling. For demonstration we consider the slot to patch array coupling in Fig.19. Slot-Patch array system considered for this purpose(see fig.19). Slot array consists of 18 identical slots with $0.4\lambda \times 0.1\lambda$. The patch array to the right consists of 9 identical patches with dimensions $0.4\lambda \times 0.2\lambda$ (inner rectangle) and $0.6\lambda \times 0.4\lambda$ (outer rectangle). Solution of this problem **required 116 Mbytes of Memory without FMM but only 11Mbytes with FMM**. All slots are excited (active) . Our goal is to observe the coupling as a function of array separation between two array systems. Fig. 20-22 show the field distribution for different separation distances. As you can see that the coupling decreases as “d” increases.

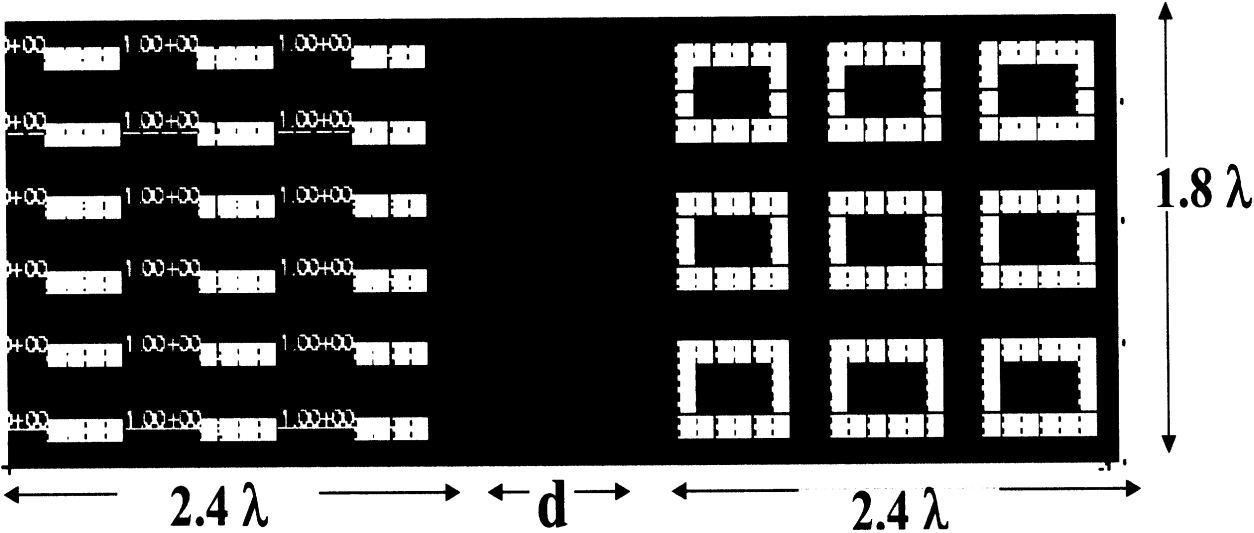


Figure 19. Geometry of the array system

MSC/PATRAN Version 9.0 23-Jul-01 00:35:45

Fringe: bistatic, MAX DEFLECTION = 0.00E+00, DISPLACEMENT, ROTATION - MAG, (NON-LAYERED)

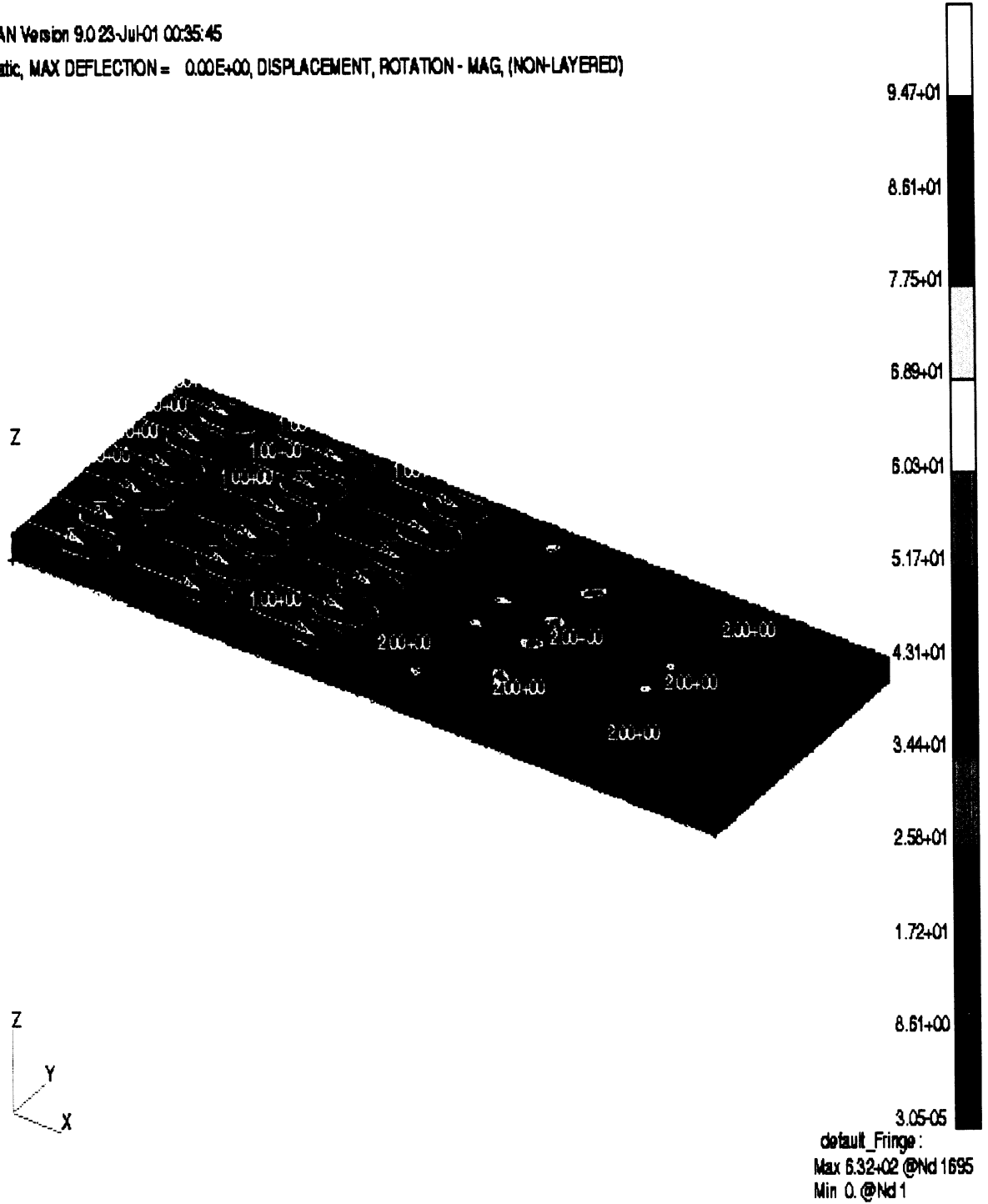


Figure 20. Field distribution $d=0.1\lambda$

MSC/PATRAN Version 9.0 23-Jul-01 03:04:36

Fringe: bistatic, MAX DEFLECTION = .00E+00, DISPLACEMENT, ROTATION - Magnitude, (NON-LAYERED)

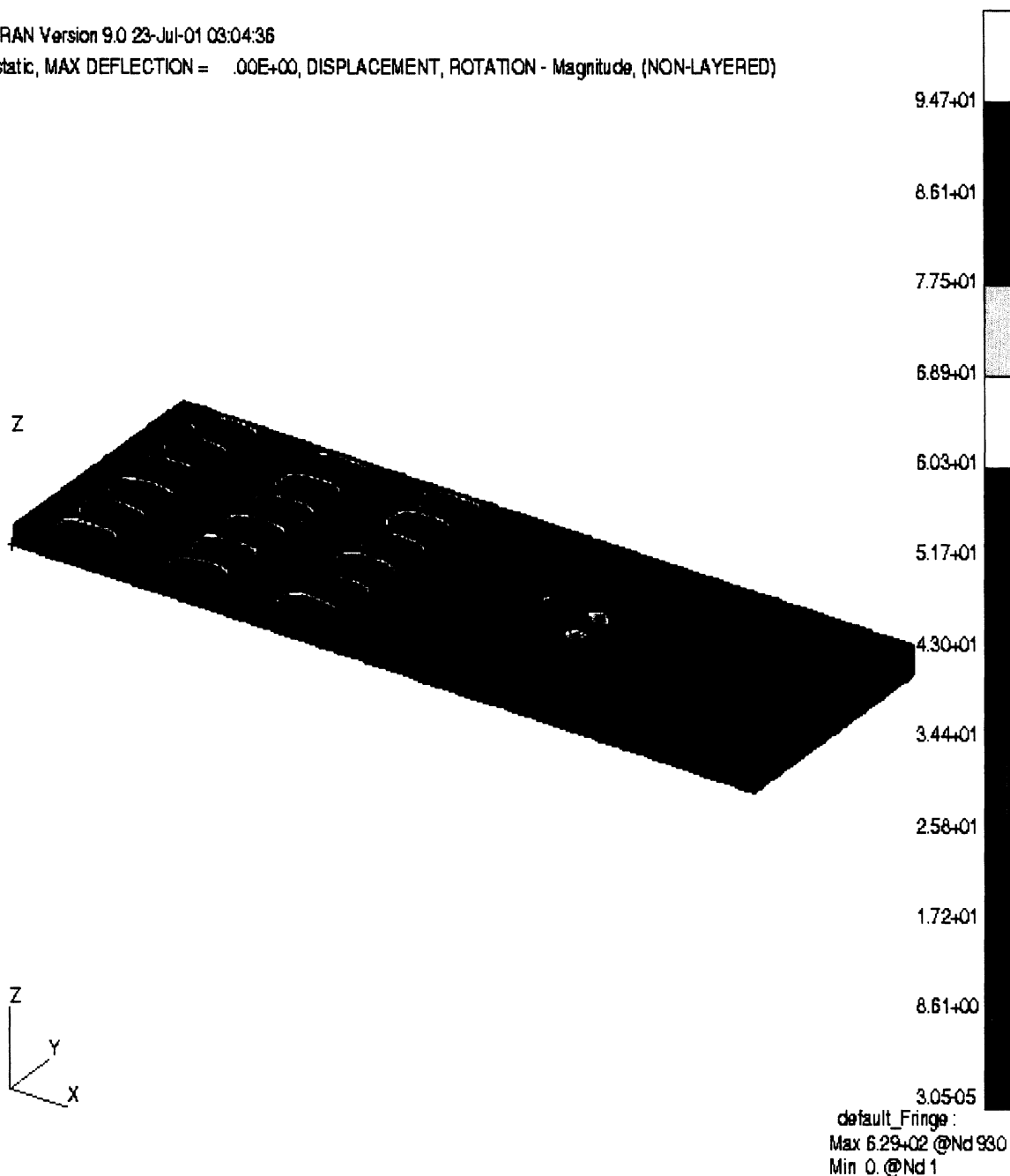


Figure 21. Field distribution $d=0.5\lambda$

MSC/PATRAN Version 9.0 23-Jul-01 14:10:09

Fringe: bistatic, MAX DEFLECTION = .00E+00_3, DISPLACEMENT, ROTATION - MAG, (NON-LAYERED)

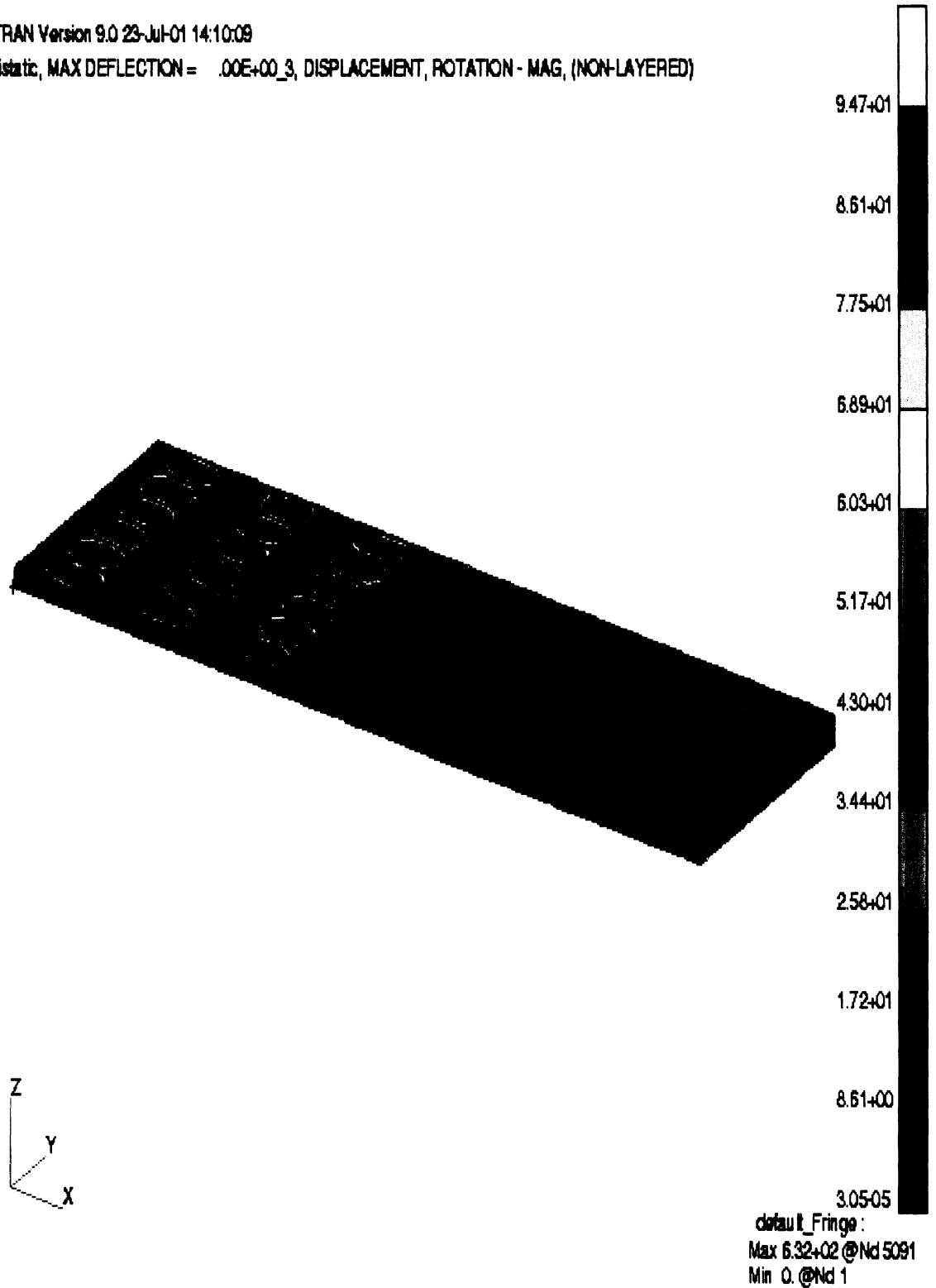


Figure 22. Field distribution $d=1\lambda$

Fig. 23-25 show the coupling from slot array to patch array elements. Element 1 is the upper left patch, element 2 is the middle left patch and 3 is the lower left patch.

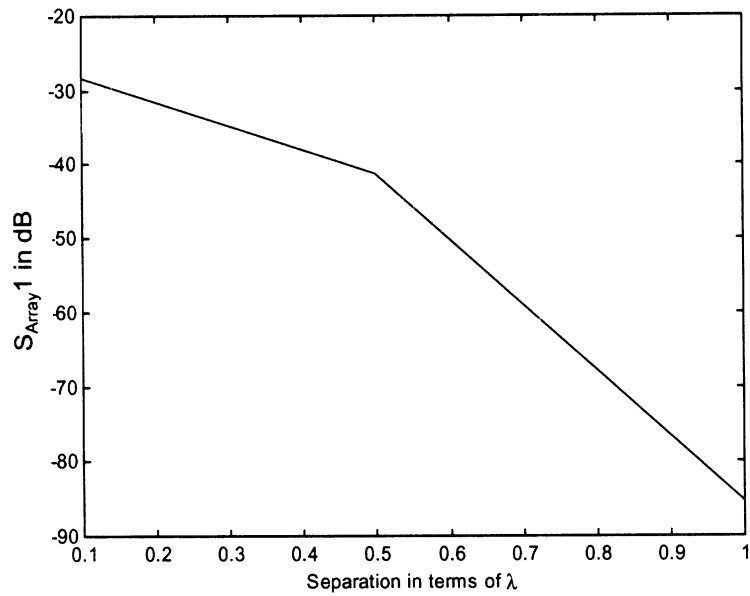


Figure 23. Coupling (array to element)

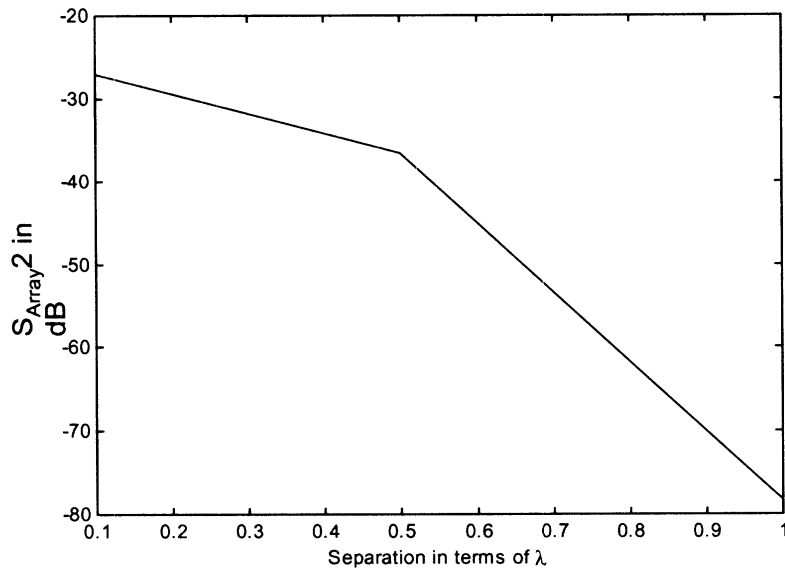


Figure 24. Coupling (array to element)

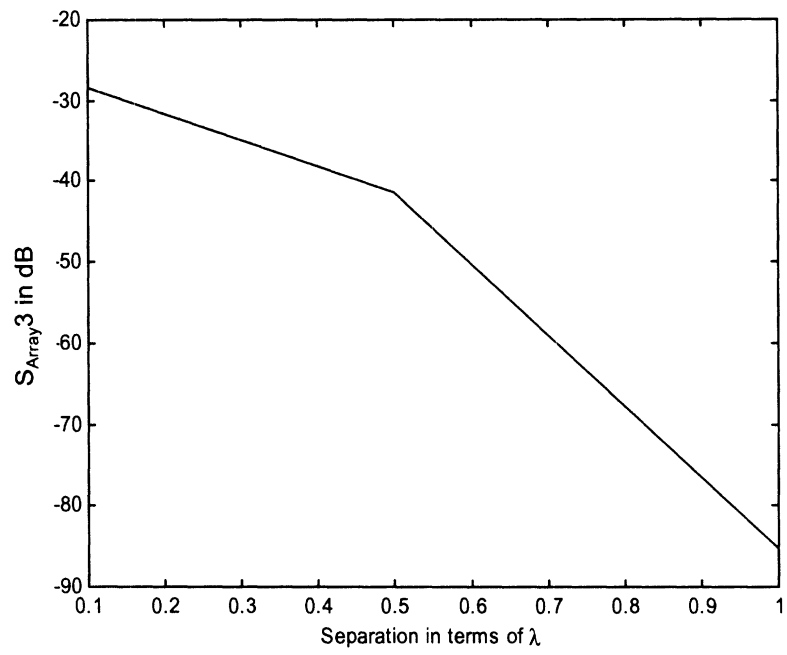


Figure 25. Coupling (array to element)

REFERENCES

[1] **Jian-Ming Jin, John Volakis**, “A hybrid Finite Element Method for Scattering and Radiation by Microstrip Patch Antennas and Arrays Residing in a Cavity”, IEEE Antennas and Propagat. Vol.39. , no.11, November 1991

[2] **Yousef Saad**, “Iterative Methods for Sparse Linear Systems”, <http://www-users.cs.umn.edu/~saad/books.html>

[3] **John Volakis, Arindam Chatterjee, Leo Kempel**, “Finite Element Method for Electromagnetics”, IEE press, 1998

[4] **Gerard L.G.Sleijpen, Diederik R. Fokkema**, “BICGSTAB(L) for Linear Equations Involving Unsymmetric matrices with Complex Spectrum”, Electronic Transactions on Numerical Analysis, vol.1, pp.11-32, September 1993

Multipoles: 25 25
 Level: 1 has 8 clusters, Max radius: 4.330127
 Multipoles: 44 44
 Number of non-zeros in M near-field matrix 29584
 Memory required for M Matrix = 0.3385543 MBytes
 Number of non-zeros in J near-field matrix 1548
 Memory required for J Matrix = 1.7715048E-02MBytes
 Total Memory for Matrix = 0.3562693 MBytes - memory saved: 0.0000000E+00%
 number of nonzeros in zbib2 matrix: 36
 Memory required for zbib Matrix = 4.1197788E-04MBytes
 FULL MATRIX SIZE = 199
 Solution completed in = 1.250000 sec.

2.2.2 Zin.txt file

This file has the input impedance data for antenna applications. The first column is the node number for the feed and the second column is the frequency in Hz. The third column is the real part of the impedance and the last column is the imaginary part of the impedance.

23	1000000000.0000	2.5928	92.3192
23	1950000000.0000	281.6845	-153.3611
23	2900000000.0000	23.9289	153.3141
23	3849999872.0000	65.7498	-5.1517
23	4800000000.0000	73.6660	308.6587
23	5750000128.0000	452.4126	546.9125
23	6700000256.0000	98.2463	66.5950
23	7649999872.0000	392.7809	464.2363
23	8600000512.0000	1267.5032	-347.5011
23	9550000128.0000	269.3477	575.8915
23	10499999744.0000	431.3055	348.6778
23	11450000384.0000	323.2536	-85.0863
23	12400000000.0000	423.1139	-663.8707
23	13349999616.0000	481.1049	-570.9062
23	14300000256.0000	253.0912	317.7504
23	15249999872.0000	338.6689	-1308.7921
23	16200000512.0000	124.3804	-706.0308
23	17150000128.0000	87.8632	-537.5041
23	18100000768.0000	64.2989	-446.8862
23	19050000384.0000	51.8515	-397.6943
23	20000000000.0000	41.8530	-354.2432

2.2.3 Solver.txt file

Convergence data is kept in this file. The first column shows the number of iteration steps, the second column gives the total solution time after each iteration. The last column is the residual error.

1	1.4375	0.0291
2	1.4844	0.0048
3	1.5156	0.0020
4	1.5469	0.0007
5	1.5938	0.0001
1	3.5781	0.0564
2	3.6250	0.0031
3	3.6562	0.0015
4	3.6875	0.0002
5	3.7344	0.0000
....		
....		
....		
....		
1	53.8438	0.1357
2	53.8750	0.1370
3	53.9062	0.0970
4	53.9375	0.0995
5	53.9688	0.0965
6	54.0000	0.1026
7	54.0312	0.0935
8	54.0625	0.0767
9	54.0938	0.1018
10	54.1250	0.1399
11	54.1562	0.1448
12	54.1875	0.1205
13	54.2031	0.1101
14	54.2344	0.4003
15	54.2656	0.0865
16	54.2969	0.0530

2.2.4 Farfield.txt file

This file contains the farfield and antenna gain data. The first column is the observation angle, the second column is the angle phi, the third column is the gain in dB, the fourth column is the $|E_{\theta}|$ in dB, the fifth column is the E_{θ} (phase), the sixth column is $|E_{\phi}|$ in dB, the seventh column is E_{ϕ} (phase) and the last column is the free space wave number.

-180.00000	0.00000	1.47751	-269.82554	154.43714	-32.36208	139.33551	0.20944
-179.00000	0.00000	1.47590	-269.79033	156.03487	-32.36368	140.37765	0.20944
-178.00000	0.00000	1.47110	-269.75294	157.62317	-32.36849	141.40947	0.20944
-177.00000	0.00000	1.46308	-269.71372	159.20093	-32.37650	142.43065	0.20944
-176.00000	0.00000	1.45186	-269.67268	160.76887	-32.38773	143.44090	0.20944
-175.00000	0.00000	1.43742	-269.63027	162.32351	-32.40216	144.43993	0.20944
-174.00000	0.00000	1.41977	-269.58665	163.86681	-32.41982	145.42744	0.20944
-173.00000	0.00000	1.39888	-269.54202	165.39741	-32.44070	146.40316	0.20944
-172.00000	0.00000	1.37476	-269.49624	166.91604	-32.46482	147.36682	0.20944
-171.00000	0.00000	1.34740	-269.44975	168.42117	-32.49219	148.31815	0.20944
-170.00000	0.00000	1.31678	-269.40276	169.91251	-32.52281	149.25692	0.20944
-169.00000	0.00000	1.28289	-269.35551	171.39113	-32.55670	150.18285	0.20944
-168.00000	0.00000	1.24572	-269.30820	172.85503	-32.59387	151.09573	0.20944
-167.00000	0.00000	1.20524	-269.26089	174.30439	-32.63435	151.99532	0.20944
-166.00000	0.00000	1.16145	-269.21399	175.74066	-32.67814	152.88141	0.20944
.....							
.....							
.....							
169.00000	90.00000	-4.17444	-14.52292	84.21229	-46.00386	97.29349	4.18879
170.00000	90.00000	-4.23721	-14.58576	87.76211	-45.96957	101.11918	4.18879
171.00000	90.00000	-4.29767	-14.64628	91.19469	-45.94393	104.81904	4.18879
172.00000	90.00000	-4.35557	-14.70424	94.50432	-45.92633	108.39607	4.18879
173.00000	90.00000	-4.41069	-14.75941	97.68561	-45.91624	111.85298	4.18879
174.00000	90.00000	-4.46281	-14.81157	100.73358	-45.91318	115.19227	4.18879
175.00000	90.00000	-4.51175	-14.86054	103.64362	-45.91673	118.41626	4.18879
176.00000	90.00000	-4.55732	-14.90614	106.41165	-45.92655	121.52712	4.18879
177.00000	90.00000	-4.59937	-14.94821	109.03404	-45.94238	124.52692	4.18879
178.00000	90.00000	-4.63777	-14.98663	111.50775	-45.96404	127.41763	4.18879
179.00000	90.00000	-4.67241	-15.02127	113.83032	-45.99142	130.20122	4.18879
180.00000	90.00000	-4.70319	-15.05205	115.99988	-46.02454	132.87960	4.18879

2.2.5 Unk.txt file

This file contains the solution of the matrix system. The first row has 3 numbers which identify to the number of nodes, number of elements and number of edges of the solved problem, respectively. Starting from the second row, the first column is the real part and the second column is imaginary part of the edge unknowns.

```
441    30    199
1.1402947E-03 -1.0822310E-02
-3.1745189E-03  2.1807922E-03
-1.6768403E-02  4.7321372E-02
 7.7323928E-03 -1.5241545E-02
 2.8104907E-02 -0.1343380
-1.1974756E-02  4.7691219E-02
-4.6135327E-03  0.3158260
-1.3691365E-03 -0.1109501
-7.6575123E-02 -0.6964256
 2.7324101E-02  0.2306932
-4.9592401E-03  0.3136652
-3.4611262E-03 -0.1103154
 2.3482572E-02 -0.1298027
-9.7154286E-03  4.8963424E-02
-1.1000624E-02  4.4037141E-02
 5.7663918E-03 -1.5348383E-02
 2.5958717E-03 -8.9949882E-03
....
....
....
-8.3478196E-03  1.0589331E-02
 6.9731385E-02 -3.7788223E-02
 3.9119616E-02 -2.1997938E-02
 8.2472537E-04 -1.6914666E-02
-2.6502043E-02  1.0057846E-03
-1.4488138E-03 -8.5019311E-03
-2.5751784E-02 -3.9097685E-03
-1.0411549E-02  1.5343880E-02
```


2.3 Plots

The following we give some results from the sample slot antenna. Fig.24 and 25 show the input impedance versus frequency. Two different meshes are used for the calculations. Coarse mesh is the one with edge length=1cm and the dense mesh is for 0.5cm. Note that coarse and dense meshes agree up to ~ 7.3 GHz which is an expected value since the edge length for that frequency in the case of coarse mesh is $\sim \lambda/5$ which is far more than $\lambda/15$ (a recommended value for FEM analysis). For frequencies < 2.5 GHz, the edge length is $< \lambda/15$ and that is the reason for almost identical results in 1-2.5GHz for 2 different meshes. Fig. 26 and 27 show the directivity in dB for E and H-planes as a function of the observation angle at 3 different frequencies.

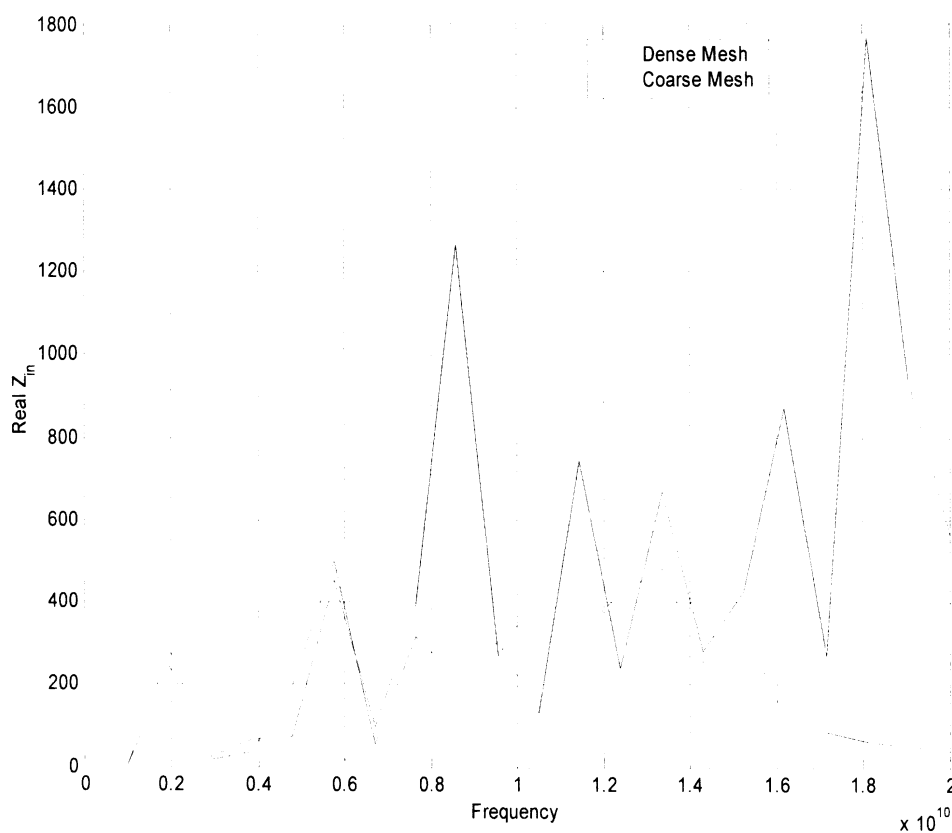


Fig. 24 Input Impedance as a function of frequency (real part)

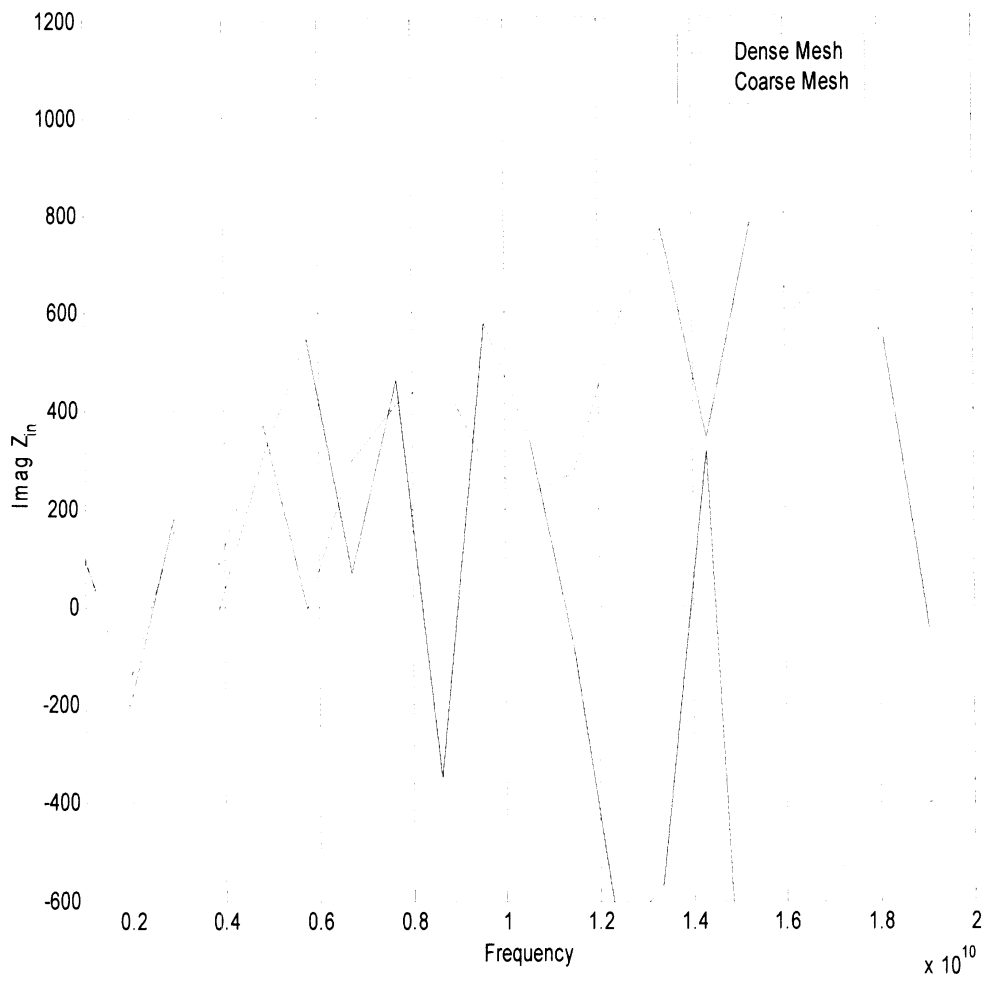


Fig. 25 Input Impedance as a function of frequency(Imaginary Part)

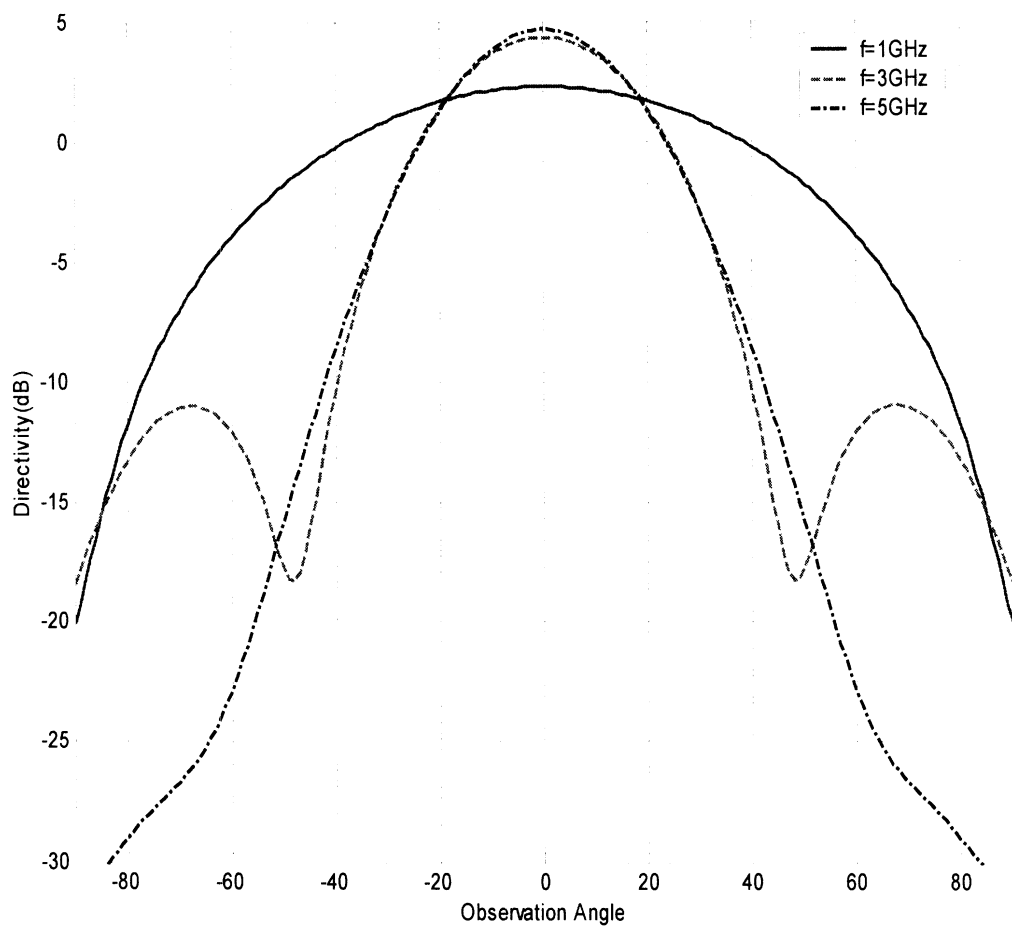


Fig. 26 Directivity as a function of observation angle (E-plane)

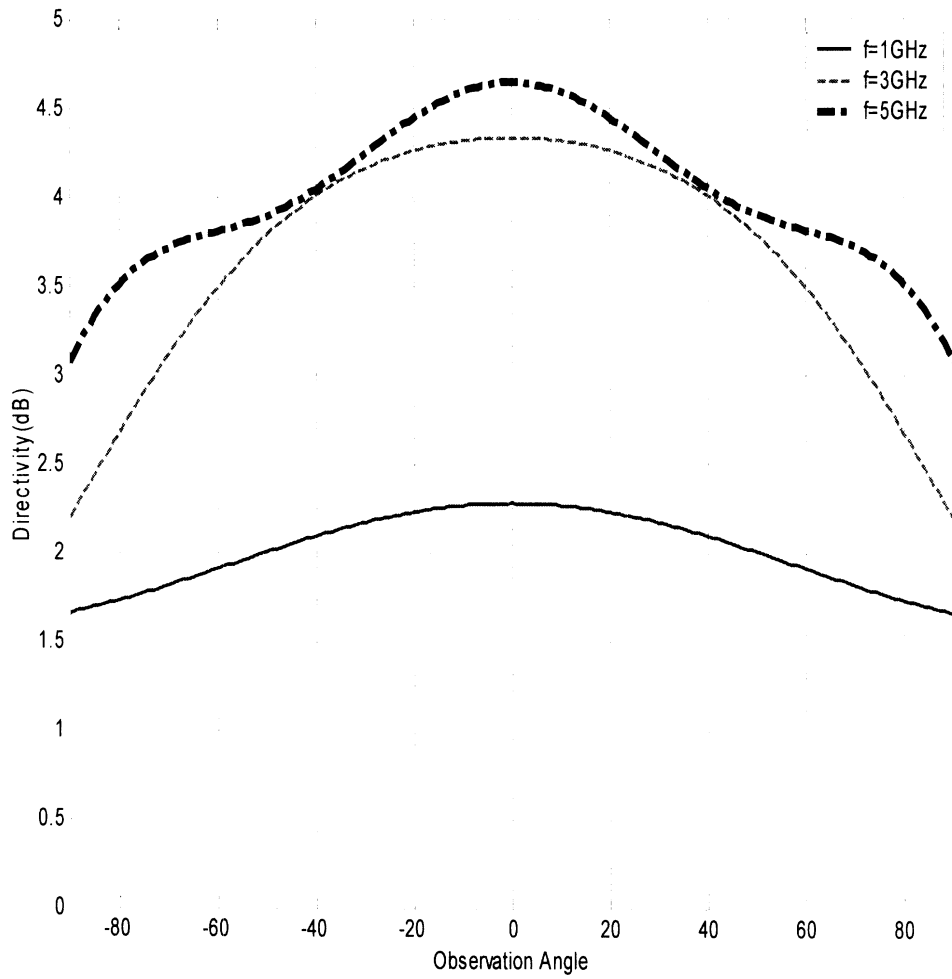


Fig. 27 Directivity as a function of observation angle (H-plane)

3. Post-Processing

In this section we are going to show how to use “Efield.txt” file to visualize fields in PATRAN. PATRAN has an “restxt.exe” file for converting “*.txt” files to “*.res” files. This executable can be found in the \bin directory. Using this file **Efield.txt** file should be converted to **Efield.res** file. Note that if you are running the code for several different frequencies the last frequency data will be kept in Efield.txt file. If needed all frequency data can be written into this file with a minor code modification but in order to visualize the results several *.txt files should be created for each frequency before using “restxt.exe”.

3.1 Importing near field data into PATRAN

After the “*.res” files have been created, they can be ported into PATRAN. Fig. 28 shows the “import window”. In the import window choose

- Object (Results)
- Format (P/FEA2.res)
- Current Analysis Code (MSCNASTRAN).

Click on the file to be imported and press the “Apply” button. To see the results click on the results icon on the viewport (see Fig. 29) and set

- Action (Create)
- Object (Fringe)
- Select Result (bistatic, MAX DEFLECTION)
- Select Fringe Result (DISPLACEMENT, ROTATION)

and “Apply”. Note that the terminology is different since PATRAN was originally written for mechanical engineering analysis.

Finally, Fig. 30 and 31 show the efield variation for 3 and 5Ghz, respectively. These are the postscript (*.ps) files exported from PATRAN using the “print to a file” option.

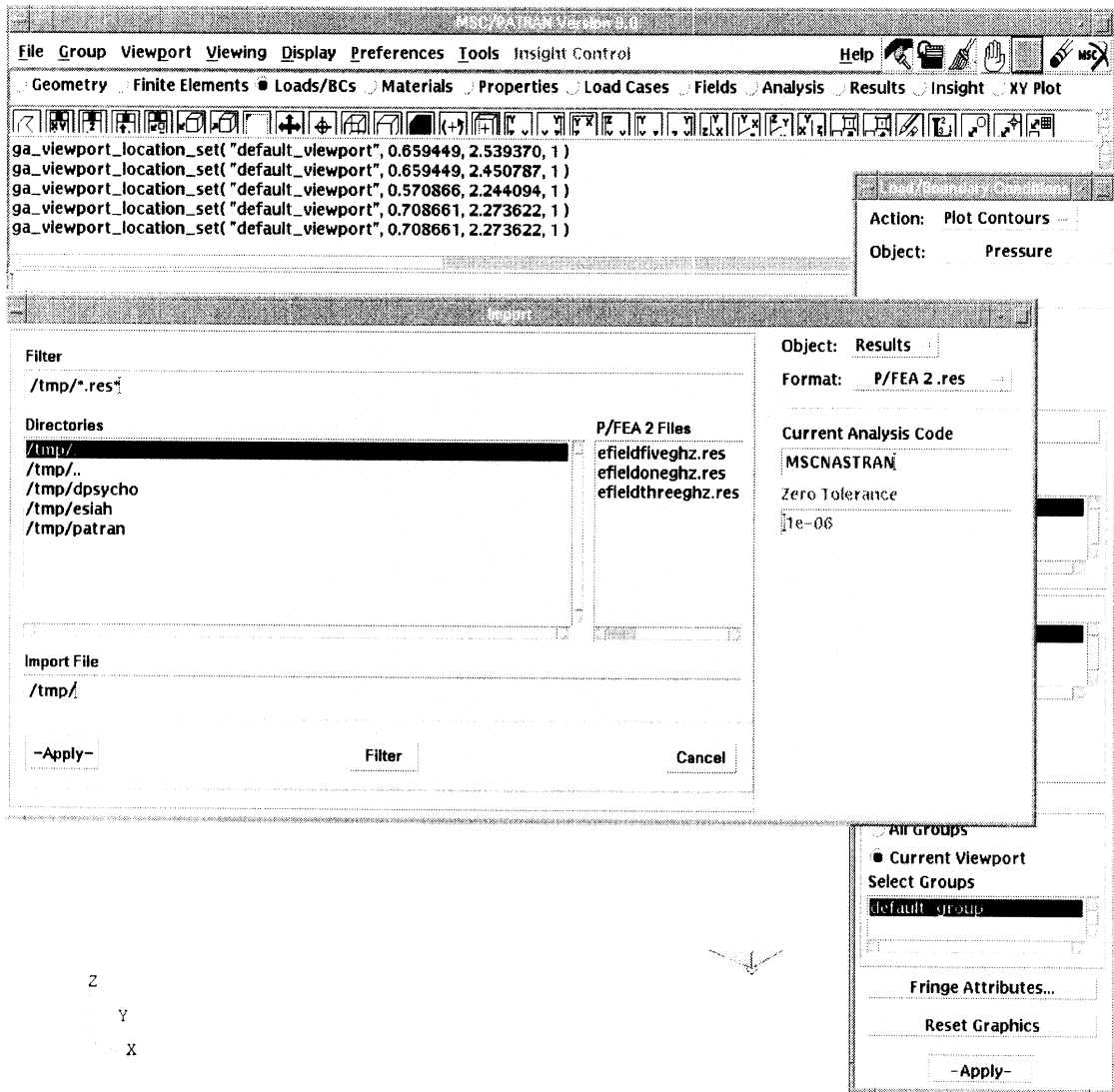


Fig. 28 Importing results data

3.2 Visualization

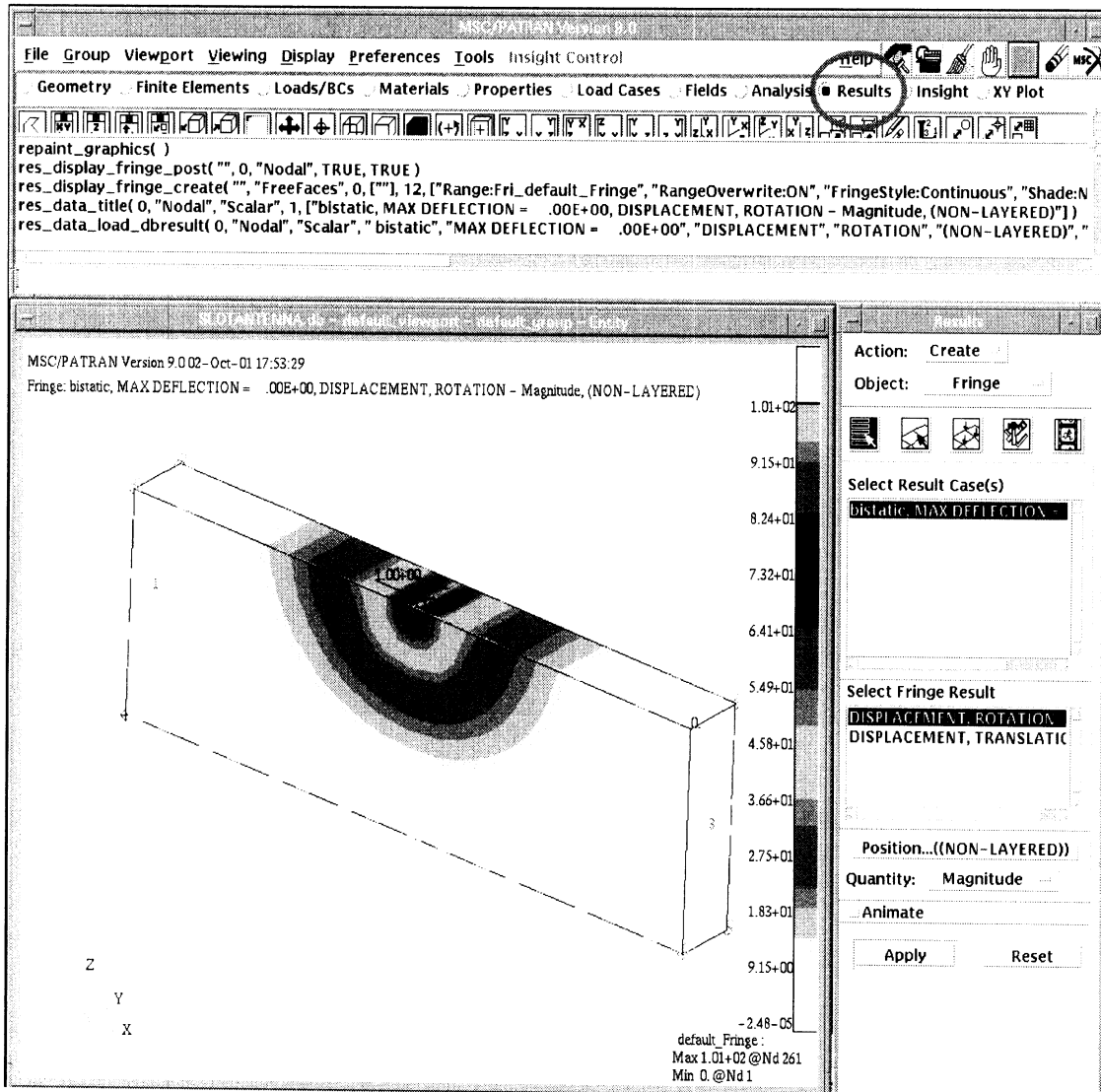


Fig. 29 Viewing the results

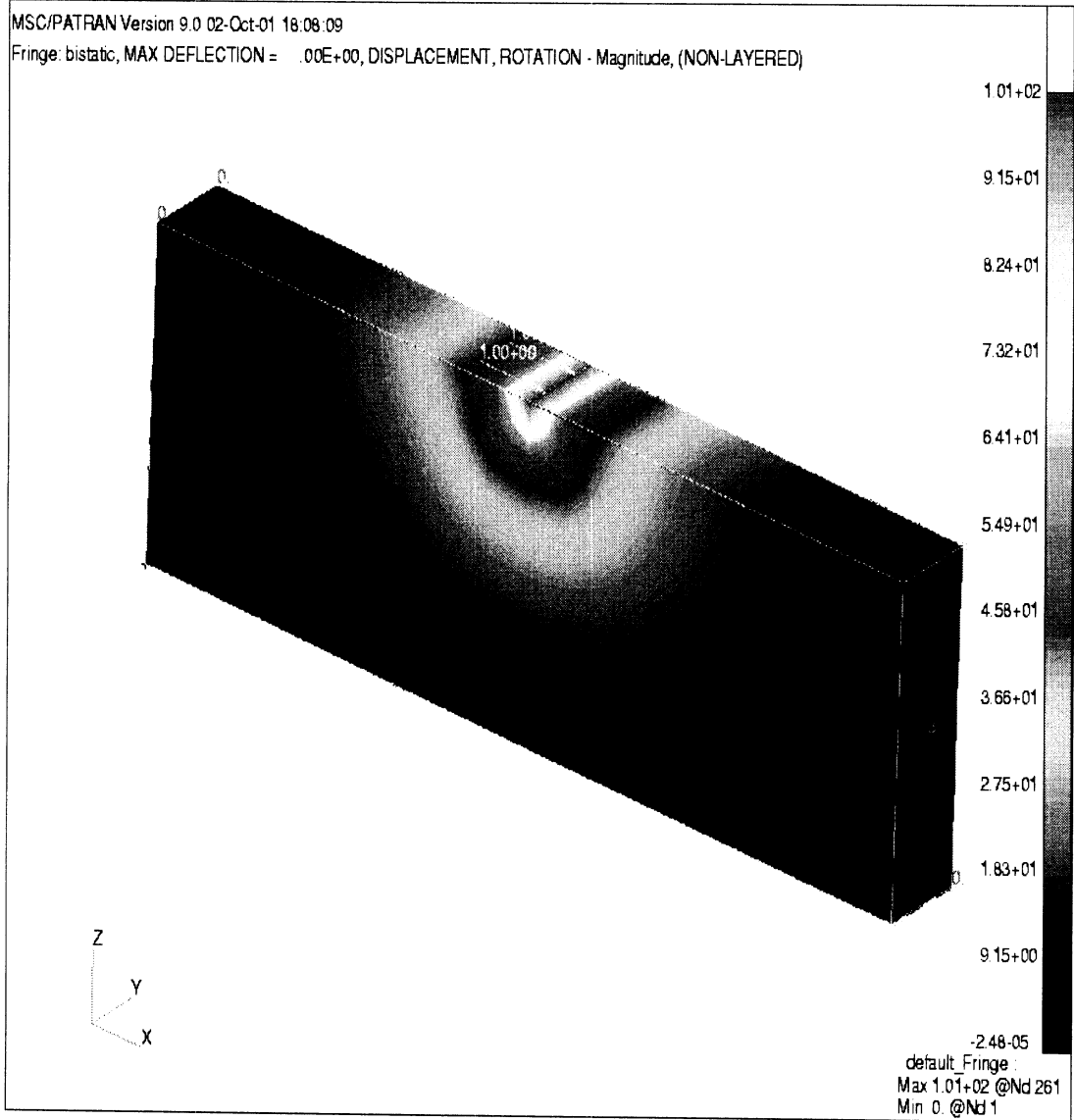


Fig. 30 E-field variation at 3-GHz

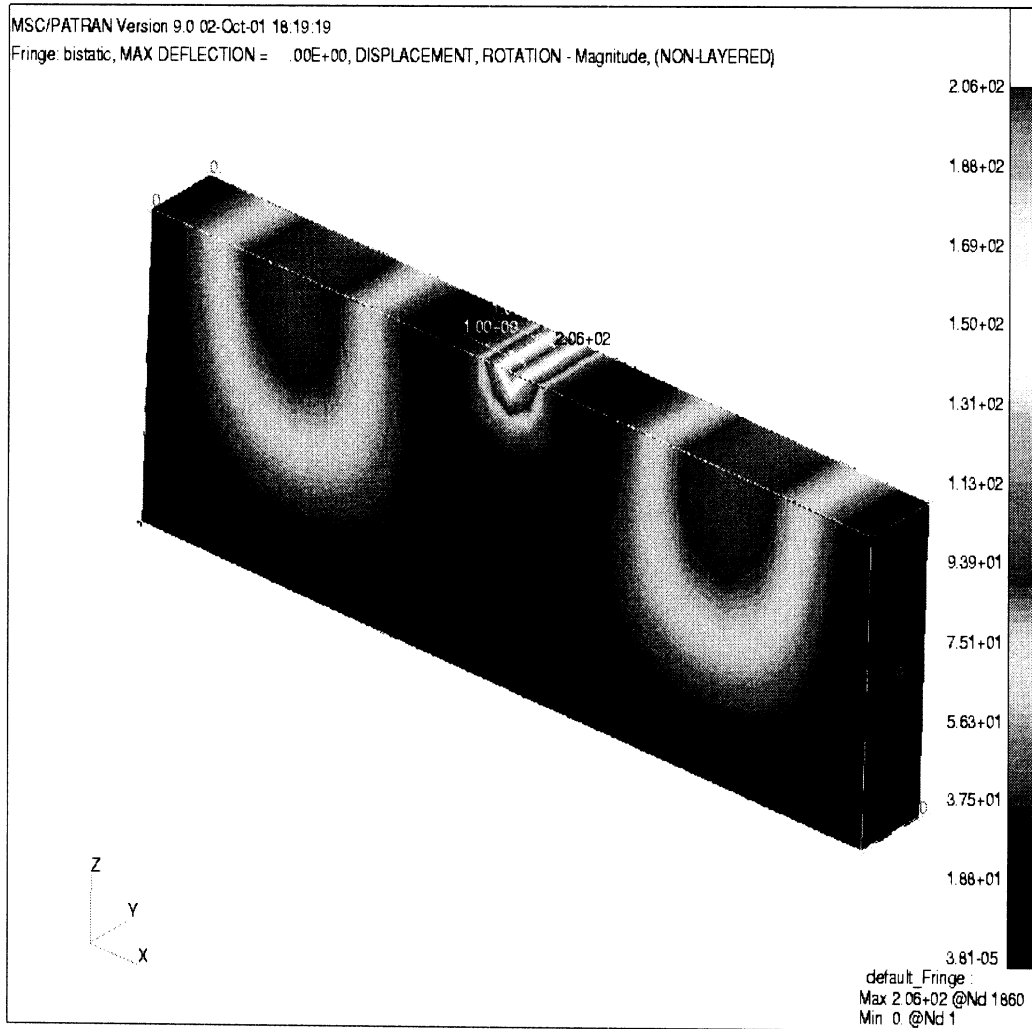


Fig. 31 E-field variation at 5-GHz

References

- [1] **K.K.Mei and J.Van Bladel**, "Scattering by perfectly conducting rectangular cylinder", IEEE Trans. Ant. Prop., AP-11, pp.185-192, March 1963.
- [2] **T.K. Wu and L.L. Tsai**, "Scattering by arbitrarily cross sectioned layered lossy dielectric cylinders," IEEE Trans. Ant. Prop., AP-25, pp. 518-524, July 1977.
- [3] **S.M. Rao, D.R. Wilton, and A.W. Glisson**, "Electromagnetic Scattering by surfaces of arbitrary shape", IEEE Trans. Ant. Prop., AP-30, pp. 409-418, May 1982.
- [4] **K.Umashankar, A. Taflove and S.M. Rao**, "Electromagnetic scattering by arbitrary shaped three dimensional homogeneous lossy dielectric objects", IEEE Trans. Ant. Prop. AP-34, pp. 758-766, June 1986.
- [5] **J.H. Richmond**, "Scattering by a dielectric cylinder of arbitrary cross-section shape", IEEE Trans. Ant. Prop., AP-13, pp.334-341, March 1965.
- [6] **J.H. Richmond**, "TE-wave scattering by a dielectric cylinder of arbitrary cross section shape", IEEE Trans. Ant. Prop., AP-14, pp. 460-464, July 1964.
- [7] **D. E. Livesay and K.M. Chen**, "Electromagnetic fields induced inside arbitrarily shaped biological bodies", IEEE Trans. Microw. Theo. Tech., MTT-22, pp. 1273-1280, Dec. 1974.
- [8] **D.H. Schaubert, D.R. Wilton and A.W. Glisson**, "A tetrahedral modeling method for electromagnetic scattering by arbitrarily shaped inhomogeneous dielectric bodies", IEEE Trans. Ant. Prop., AP-32, pp. 77-85, Jan. 1984.
- [9] **Jian-Ming Jin, John Volakis, Jeffery D. Collins**, "A Finite-Element Boundary Integral Method for Scattering and Radiation by Two- and Three- Dimensional Structures", IEEE Antennas and Prop. Magazine, Vol.33, No.3, June 1991
- [10] **Jian-Ming Jin, John Volakis**, "A Hybrid Finite Element Method for Scattering and Radiation by Microstrip Patch Antennas Residing in a Cavity", IEEE Trans. on Antennas and Prop., vol. 39, no.11, November 1991
- [11] **Erdem Topsakal, Rick Kindt, Kubilay Sertel, John Volakis**, " Input Impedance Characteristics of LTSA antennas, IEEE Antennas and Propagation Society, International Symposium, Boston, Massachusetts July 9- 13, 2001
- [12] **John Volakis, A. Chatterjee, Leo Kempel**, " Finite Element Methods for Electromagnetics", IEEE Press, New York, 1998
- [13] **Coifman, R., V. Rokhlin, and S. Wandzura**, "The fast multiple method for the wave equation: A pedestrian prescription", IEEE Antennas and Propag. Mag. 35(3), 7-12, 1993